Chemical Technology Division
Chemical Technology Division
Chemical Technology Division
Chemical Technology Division
Chemical Technology Division
Chemical Technology Division
Chemical Technology Division
Chemical Technology Division
Chemical Technology Division
Chemical Technology Division
Chemical Technology Division
Chemical Technology Division
Chemical Technology Division
Chemical Technology Division
Chemical Technology Division
Chemical Technology Division
Chemical Technology Division

ANL-94/47

Development Program for Magnetically Assisted Chemical Separation: Evaluation of Cesium Removal from Hanford Tank Supernatant

by L. Nuñez, B. A. Buchholz, M. Ziemer, G. Dyrkacz, M. Kaminski, G. F. Vandegrift, K. J. Atkins, F. M. Bos, G. R. Elder, and C. A. Swift

Argonne National Laboratory, Argonne, Illinois 60439
operated by The University of Chicago
for the United States Department of Energy under Contract W-31-109-Eng-38

Chemical Technology Division
Chemical Technology Division
Chemical Technology Division
Chemical Technology Division

Reproduced from the best available copy.

Available to DOE and DOE contractors from the
Office of Scientific and Technical Information
P.O. Box 62
Oak Ridge, TN 37831
Prices available from (615) 576-8401

Available to the public from the
National Technical Information Service
U.S. Department of Commerce
5285 Port Royal Road
Springfield, VA 22161

Distribution Category:
Defense Waste Management
(UC-721)

ANL – 94/47

Argonne National Laboratory
9700 South Cass Avenue
Argonne, Illinois 60439

DEVELOPMENT PROGRAM FOR MAGNETICALLY ASSISTED CHEMICAL SEPARATION: EVALUATION OF CESIUM REMOVAL FROM HANFORD TANK SUPERNATANT

Principal Investigators

L. Nuñez, B. A. Buchholz, M. Ziemer,
G. Dyrkacz, M. Kaminski, and G. F. Vandegrift

Argonne National Laboratory
Chemical Technology and Chemistry Divisions

and

K. J. Atkins, F. M. Bos, G. R. Elder, and C. A. Swift

Bradtec, Inc.

Contract No. 31682401

December 1994

TABLE OF CONTENTS

TABLE OF CONTENTS (contd)

DEVELOPMENT PROGRAM FOR MAGNETICALLY ASSISTED CHEMICAL SEPARATION: EVALUATION OF CESIUM REMOVAL FROM HANFORD TANK SUPERNATANT

(L. Nuñez, B. A. Buchholz, M. Ziemer, G. Dyrkacz, M. Kaminski, G. F. Vandegrift, K. J. Atkins, F. M. Bos, G. R. Elder, and C. A. Swift)

ABSTRACT

Magnetic particles (MAG*SEP^{SM}) coated with various absorbents were evaluated for the separation and recovery of low concentrations of cesium from nuclear waste solutions. The MAG*SEP^{SM} particles were coated with (1) clinoptilolite, (2) transylvanian volcanic tuff, (3) resorcinol formaldehyde, and (4) crystalline silico-titanate, and then were contacted with a Hanford supernatant simulant. Particles coated with the crystalline silico-titanate were identified by Bradtec as having the highest capacity for cesium removal under the conditions tested (variation of pH, ionic strength, cesium concentration, and absorbent/ solution ratio). The MAG*SEP^{SM} particles coated with resorcinol formaldehyde had high distribution ratios values and could also be used to remove cesium from Hanford supernant simulant.

Gamma irradiation studies were performed on the MAG*SEP^{SM} particles with a gamma dose equivalent to 100 cycles of use. This irradiation decreased the loading capacity and distribution ratios for the particles by greater than 75%. The particles demonstrated high sensitivity to radiolytic damage due to the degradation of the polymeric regions. These results were supported by optical microscopy measurements. Overall, use of magnetic particles for cesium separation under nuclear waste conditions was found to be marginally effective.

SUMMARY

The Magnetically Assisted Chemical (MACS) Separation Program seeks to develop a process that will combine the selectivity afforded by ion exchange and magnetic separation and provide a more efficient chemical separation for transuranics, radionuclides, and heavy metals in nuclear waste solutions. Bradtec, Inc., and Argonne National Laboratory have joined efforts to develop magnetic particles coated with absorbents selective for cesium removal. This report focuses on the feasibility of the separation process for removing cesium from Hanford tank supernatant. This effort is detailed in a two-part report describing Bradtec and ANL tasks separately.

Magnetic (MAG*SEP^{SM}) particles with an absorbed layer of (1) clinoptilolite (75-200 μm), (2) transylvanian volcanic tuff (100-450 μm), (3) resorcinol formaldehyde (100-450 μm), and (4) crystalline silico-titanate (100-450 μm) were evaluated for recovery of cesium from Hanford supernatant simulant. Particles were tested by varying (1) solution ionic strength, (2) cesium concentration, (3) solution pH, and (4) magnetic particle-to-solution ratios for a simulant of average Hanford tank supernatant. The contact time used for the simulant solutions

was 15 min and consistent with the requirements of the MAG*SEP^{SM} process; however, this was much shorter than the 17 to 72 h needed to reach chemical equilibrium. Thus, the distribution ratios (K_d) in this report reflect kinetic rate measurements and not equilibrium distributions. The highest K_d values were observed for the crystalline silico-titanate when the simulant was diluted in volume by one-fifth the original concentration; these K_d values ranged between 350 and 820. Reduction of the cesium concentration to one-tenth the original simulate composition and the hydroxide concentration to 1M resulted in poor K_d values (<100 except for silico-titanate, which ranged from 100 to 320): for most of the materials and conditions studied, K_d values <300 were obtained.

Gamma irradiation studies were performed on the MAG*SEP^{SM} particles with a gamma dose equivalent to 100 cycles of use. The particles subjected to gamma irradiation showed a substantial decrease in the capacity for cesium removal. With the original waste supernatant, K_d values dropped from 100 to 22 for the crystalline silico-titanate particles at 9.7 Mrad. With the same type of particles under similar irradiation conditions but with the supernatant solution being one-fifth of the original concentration, the K_d values dropped from 500 to 130. Optical microscopy of the crystalline silico-titanate particles showed a drastic increase in the particle size (up to 1000-12,000 μm) due to aggregation. The resulting lower surface area significantly decreased the extraction efficiency. Evidence of fine particles and polymeric unraveling was apparent in all the irradiated materials.

The chemical and physical studies performed in this evaluation indicate that cesium removal using magnetic particles is only marginally effective when compared with more traditional separation techniques.

PART ONE.

EVALUATION OF CESIUM REMOVAL FROM HANFORD TANKS

(K. J. Atkins,* F. M. Bos,* G. R. Elder,* and C. A. Swift*)

I. INTRODUCTION

The MAG*SEP^{SM} process (patent pending) developed by Bradtec, Inc., allows the selective extraction of ions from solution. The process uses magnetic particles that are chemically engineered to have surface adsorption sites tailored for specific functions. The particles are contacted with the waste stream, where they adsorb the contaminant of interest. Conventional magnetic separation technology may be employed to remove the MAG*SEP^{SM} particles from the waste stream. The fate of the MAG*SEP^{SM} particles is determined by both economic and practical considerations. The MAG*SEP^{SM} particles themselves may become the final waste form in some applications, or alternatively, they could be regenerated, enabling the contaminant to be removed from the waste stream and the "cleaned " particles to be recycled if required.

The MAG*SEP^{SM} technology is being evaluated for several projects where conventional ion exchange methods are not practical or cost effective. These projects include treatment of heavy metals and radionuclides in groundwater and wastewater.[1]

The key element of the technology is the selective adsorption particle. These composite particles consist of a magnetic core, a polymer coating for durability, and either a "functionalized" resin coating or selective seed materials embedded in the polymer coating.

Supernatants stored in the underground storage tanks at the Hanford site contain radioactive Cs and Sr, and in some cases, low concentrations of transuranics (TRUs). Bradtec has undertaken to demonstrate the feasibility of using the MAG*SEP^{SM} technology for the selective removal of cesium from the Hanford tank supernatant. A simulant waste solution is used since the actual supernatant is not available.

The work discussed in this report describes the testing performed to identify the most promising MAG*SEP^{SM} particle coating in a simulant supernatant while varying (1) solution ionic strength, (2) cesium concentration, (3) solution pH, and (4) magnetic particle-to-solution ratios.

---

*Bradtec, Inc.

II. SCOPE OF THE WORK

The demonstration of the MAG*SEP^{SM} technology for the selective removal of cesium from Hanford tank supernate simulant involved the testing of four materials for their adsorption characteristics: (1) clinoptilolite, (2) transylvanian volcanic tuff (TVT), (3) resorcinol formaldehyde (resorcinol), and (4) crystalline silico-titanate (CST). Clinoptilolite and TVT are naturally occurring zeolites and were selected because their cation exchange capacities for cesium have been successfully demonstrated in other MAG*SEP^{SM} applications. Resorcinol and CST were chosen for their high selectivity and separation capabilities for cesium in high alkaline and sodium concentrations. The composition of the Hanford waste is summarized in Table II-1.

Table II-1. Components of Hanford Simulant Waste Solution

Major Components	Component Charge	Concentration, mol/L
Na	1	8.83
K	1	9.35×10^{-2}
Cs	1	4.88×10^{-5}
OH	-1	6.54
NO_3	-1	1.09
NO_2	-1	8.09×10^{-1}
$Al(OH)_4$	-1	2.06×10^{-2}
CO_3	-2	2.22×10^{-1}
CrO_4	-2	4.37×10^{-3}
PO_4	-3	8.00×10^{-4}

Two additional materials were originally included in the study, potassium cobalt hexacyanoferrate and sodium cobalt dicarbolide, but were later removed. Potassium cobalt hexacyanoferrate has detrimental waste management implications, and cobalt dicarbolide was found to be too soluble in aqueous solutions to prepare MAG*SEP^{SM} particles.

The four candidate materials were tested for absorption capacity in powder form before the MAG*SEP^{SM} particles were prepared. Next, the adsorption characteristics of the coated particles were determined. The efficiency of the MAG*SEP^{SM} particles were measured by the distribution ratio, K_d, where K_d = [Cs-137] adsorbent per gram/[Cs-137] treated solution per milliliters. Coated particles were then irradiated with a gamma dose equivalent of 10 and 100 cycles (discussed in Part Two of this report), and the adsorption characteristics of the most promising particles were compared with the adsorption prior to irradiation. (The irradiation doses were discussed with Argonne National Laboratory and agreed to by Bradtec and Argonne.)

The contact time between the MAG*SEP^{SM} particles and the simulant waste solutions was 15 min, which is consistent with the needs for the MAG*SEP^{SM} particles. This time is significantly shorter than the 12 to 72 h normally used to obtain a distribution ratio. Consequently, the term "distribution ratio" here may be more correctly defined as a kinetic rate measurement. It is quite possible that longer contact times would produce higher K_d values (equilibrated conditions).

Some additional tests to those outlined in the contract requirements were performed to provide a baseline for the behavior of the MAG*SEP^{SM} particles. The solution prepared for these tests contained only cesium and cesium-137 (as a tracer) in deionized water. These tests permitted

the capacity of the MAG*SEP^{SM} particles to be determined. The capacity of the MAG*SEP^{SM} particles for cesium removal before irradiation was also compared with that after irradiation.

Details of the test program are as follows:

1. Select possible candidate adsorbing materials.
2. Test the candidate adsorbing materials with the Hanford simulant waste solution prepared according to Table II-1.
3. Prepare MAG*SEP^{SM} particles.
4. Perform testing with the MAG*SEP^{SM} particles according to the matrix in Table II-2.
5. Calculate K_d for cesium for each type of adsorbent and MAG*SEP^{SM} particle.
6. Send the most promising materials to ANL for irradiation testing at a gamma dose equivalent to 10 and 100 cycles of use.
7. Re-test the irradiated particles under the optimum conditions determined from the data obtained in step 5.

Table II-2. Test Matrix for MACS Testing

Experimental Variable	Maximum	Minimum
Two ionic strengths	Composition as Table II-1	Dilution by water to 1/5 of the above composition
Two Cs^+ concentrations	Composition as Table II-1	1/10 of the above composition
Two OH^- concentrations	Composition as Table II-1	Approx. 1M with $[Na^+]$ kept constant using $NaNO_3$ and $NaNO_2$ in their molar ratio given in Table II-1.
Two adsorbent/solution ratios[a]	0.05 g/mL[b]	0.005 g/mL[b]

[a]In cases where the quantity of MAG*SEP^{SM} particles was insufficient to permit both adsorbent/solution ratios to be tested, the minimum value was chosen.
[b]Concentration of MAG*SEP^{SM} particles in solution.

III. METHODOLOGY

The following adsorber materials were selected for the preparation of MAG*SEP^{SM} particles:

1. Activated transylvanian volcanic tuff
2. Clinoptilolite (particle size < 75 μm to > 45 μm)
3. Resorcinol formaldehyde
4. Crystalline silico-titanate

The clinoptilolite and TVT were supplied by Imperial College, London; crystalline silico-titanate was supplied by Norman Brown, Sandia National Laboratories, Albuquerque, NM; and resorsinol formaldehyde was supplied by J. Bibler, Westinghouse Savannah River Co., Aiken, SC.

Prior to testing, the TVT was "activated" by heating at 150°C for 24 hours.[8] The mechanism of "activation" is not clear but may involve the liberation of moisture from active sites within the zeolite.

Clinoptilolite was chosen as a possible adsorber material for cesium removal from Hanford supernatant because MAG*SEP^{SM} particles containing clinoptilolite had been used earlier by Bradtec to remove cesium from contaminated milk. The clinoptilolite was sieved into three fractions with particles in the following ranges: (1) <180 μm and >75 μm, (2) <75 μm and >45 μm, and (3) <45 μm. Tests on all three fractions using the simulant waste stream were performed to determine the optimum particle size for preparation of the MAG*SEP^{SM} particles. Resorcinol formaldehyde and crystalline silico-titanate were used as supplied, and size distribution data are available from microscopy analyses performed at ANL (see Part Two).

With some of the adsorber materials, the minimum size attainable for the MAG*SEP^{SM} particles was between 106 and 420 μm. Therefore, for consistency, all the MAG*SEP^{SM} particles used for this study were between 106 and 420 μm. The MAG*SEP^{SM} particles prepared using activated TVT were re-activated and tested in order to determine whether the process of preparing the particles adversely affected the adsorption capability. The tests showed no significant difference, and consequently, the MAG*SEP^{SM} particles were not reactivated after preparation.

The testing at Bradtec was performed according to the test procedures provided in Appendix A.

IV. RESULTS AND DISCUSSION

A. Distribution Ratio for Adsorbents before Incorporation into MAG*SEP^{SM} Particle

Testing was performed on the following types of adsorbent materials before their incorporation into a MAG*SEP^{SM} particle:

1. Powdered TVT
2. Clinoptilolite (particle size < 180 μm > 75 μm)

2a. Clinoptilolite (particle size < 75 μm > 45 μm)

2b. Clinoptilolite (particle size < 45 μm)

3. Resorcinol formaldehyde

(Note: crystalline silico-titanate was unavailable for testing at this point in the test program.) The results from the testing using the above materials are given in Table IV-1. The calculation used to

Table IV-1. Distribution Ratios for Adsorbent before Incorporation into MAG*SEP^{SM} Particles

Adsorbent	Sample A[a]	Sample B[a]
Powdered TVT	6	7
Clinoptilolite (particle size < 180 μm > 75 μm)	2	1
Clinoptilolite (particle size < 75 μm > 45 μm)	5	4
Clinoptilolite (particle size < 45 μm)	3	1
Resorcinol formaldehyde	22	15

[a]Samples A and B are duplicates.

determine the K_d values, the raw data for this testing, and the associated statistics are provided in Appendices A and B. Details pertaining to the gamma spectrometer used for the testing are provided in Appendix C.

The results in Table IV-1 show that resorcinol formaldehyde was more selective for cesium under these conditions. Clinoptilolite with a particle size of > 45 μm to < 75 μm showed a small improvement in the K_d for cesium over the two other samples of clinoptilolite studied. Consequently, clinoptilolite with this size of particles was used to prepare the MAG*SEP^{SM} particles.

B. Distribution Ratio for MAG*SEP^{SM} Particles with Varying Experimental Conditions

The testing using the powdered adsorber materials confirmed that cesium was removed, with varying efficiency, from the Hanford supernant simulant with the composition given in Table II-1. Subsequently, MAG*SEP^{SM} particles were prepared for further testing. Crystalline silico-titanate was received during this period and, therefore, was also tested. After preparation, the silico-titanate particles were examined under a microscope (see Part Two of this report), and the particle size was determined to be approximately between 106 μm and 420 μm. However, due to the irregular shape of the particles (i.e., some cylindrical particles may be present) and their tendency to "stick" together as a result of electrostatic charges, the separation of the particles into

distinct size boundaries using the current equipment was not possible. Thus, the four test materials (106 μm < particle size < 420 μm) are

1. Activated TVT MAG*SEP^{SM}
2. Clinoptilolite MAG*SEP^{SM}
3. Resorcinol formaldehyde MAG*SEP^{SM}
4. Silico-titanate MAG*SEP^{SM}

In most cases, insufficient particles were available to permit triplicate tests at the maximum particle-to-solution ratio (0.05 g/mL); therefore, in those cases, only the minimum ratio (0.005 g/mL) was used.

The K_d results for the MAG*SEP^{SM} particles with varying experimental conditions are presented in Table IV-2. The calculation used to determine the K_d values, the raw data for this testing, and the associated statistics are provided in Appendices A and B. Details pertaining to the gamma spectrometer used for the testing are provided in Appendix C.

The results in Table IV-2 show that, with the exception of clinoptilolite, the K_d value was the highest for the adsorbers tested when the simulant was diluted by one-fifth. Of these three types of MAG*SEP^{SM} particle, the highest K_d was achieved for the silico-titanate coated particles. As expected, when the concentration of competing species was reduced (condition B in Table IV-2), the K_d increased. The K_d further increased when the higher particle-to-solution ratio (0.05 g/mL) was used. Again, as expected, the K_d was significantly reduced when the cesium concentration was reduced by one-tenth (condition C). The MAG*SEP^{SM} particles coated with resorcinol formaldehyde and used in a supernatant diluted by one-fifth demonstrated the second highest K_d. When the hydroxide concentration was reduced to 1M (condition D), the K_d was highest for clinoptilolite. This behavior is consistent with clinoptilolite being more soluble in higher concentrations of hydroxide. Hence, for the tests performed in 1.8M and 8.9M hydroxide (conditions A to C), sufficient clinoptilolite may have dissolved from the particle to affect the K_d.

Comparing the results from Tables IV-1 and IV-2 shows that the K_d was not reduced significantly by incorporating the powdered adsorbents into MAG*SEP^{SM} particles. This is because the exchange process is diffusion limited, and therefore, a large improvement in K_d may only be observed if the solution is left in contact with the particles or powder for a considerable time, i.e., 24 h or more, to allow diffusion and achieve equilibrium. Hence, for the short contact time used in this testing, both the powdered adsorbent and the MAG*SEP^{SM} particles were limited to a surface adsorption mechanism only. Consequently, a large difference in K_d was not expected. In fact, the K_d values for the MAG*SEP^{SM} particles coated with resorcinol formaldehyde and clinoptilolite were, on average, improved over the tests with the powdered materials, although still of the same order of magnitude.

The Hanford tank waste simulant (Table II-1) consisted of 8.8M Na^+ and 6.54M OH^-. These concentrations are considerably higher than most Hanford simulants, where the Na^+ concentration is typically between 5 and 6M and the OH^- concentration is between 1 and 2M. As a consequence, the simulant in this study has a higher viscosity, slower exchange kinetics, and greater competition between Na^+ and Cs^+.

The combined effect of the higher Na^+ concentrations, together with the short contact times used for the study, resulted in much lower K_d values than reported elsewhere.[3] Other factors affecting the K_d are discussed later.

Table IV-2. Distribution Ratios Obtained for MAG*SEP^{SM} Particles (0.05 and 0.005 g/mL) with Varying Experimental Conditions[a]

	A		B		C		D	
	0.05[b]	0.005[b]	0.05[b]	0.005[b]	0.05[b]	0.005[b]	0.05[b]	0.005[b]
Activated TVT MAG*SEP^{SM}	4	-	-	23	-	0	-	4
	2	-	-	22	-	21	-	16
	-	-	-	39	-	0	-	6
Resorcinol Formaldehyde MAG*SEP^{SM}	-	39	-	136	-	168	-	0
	-	58	-	161	-	65	-	5
	-	43	-	364	-	0	-	13
Crystalline Silico-titanate MAG*SEP^{SM}	49	108	820	353	-	53	-	278
	64	102	421	685	-	81	-	320
	-	-	-	369	-	141	-	100
Clinoptilolite MAG*SEP^{SM}	-	0	-	54	-	3	-	100
	-	11	-	76	-	30	-	73
	-	20	-	41	-	113	-	63

[a]Conditions:
A = Waste solution simulant as given in Table II-1.
B = Waste solution simulant as given in Table II-1 diluted by one-fifth.
C = Waste solution simulant with the cesium concentration reduced by one-tenth.
D = Waste solution simulant with the hydroxide concentration reduced to 1M.
[b]Weight of MAG*SEP^{SM} in solution, g/mL.

C. Effect of Gamma Irradiation

The capacity of the MAG*SEP^{SM} particles, prior to irradiation, was determined by using a solution of inert cesium containing a trace amount of cesium-137 (baseline solution) and is reported in milliequivalent per gram (meq/g). The minimum particle-to-solution ratio was used for this study, i.e., 0.005 g of MAG*SEP^{SM} particles per milliliter of solution.

The baseline solution was prepared as follows: 0.1065 g of cesium bromide was dissolved in 500 mL of deionized water to give a solution containing 1 mM inert cesium. To this solution, 5 kBq (1.35×10^{-7} Ci) of Cs-137 was added as a tracer. At a specific activity for Cs-137 of 9.8 Ci/g, 5 kBq equates to 1.38×10^{-8} g or 2×10^{-10}M Cs. Hence, due to the insignificant concentration of Cs-137 tracer present, the effective molarity of cesium in the solution was 1 mM. The MAG*SEP^{SM} particles were contacted with the solution for 15 min.

The particles were re-tested after irradiation to a gamma dose equivalent to 100 cycles, and the results were used to assess the effect of irradiating the particles on the cesium capacity. (Note: this testing was performed with particles that had been irradiated with a high gamma dose as a "worst case" scenario.)

The effect of radiation dose on the cesium capacity of MAG*SEP^{SM} particles is shown in Table IV-3. The MAG*SEP^{SM} particles coated with resorcinol formaldehyde were the least affected (15% reduction of their original capacity), while particles coated with clinoptilolite were the most affected (36% reduction in capacity). However, the capacity of the clinoptilolite particles may also have been reduced by contact with the supernatant during the irradiation, resulting in the partial dissolution of the clinoptilolite.

Table IV-3. Results for the MAG*SEP^{SM} Particle Capacity for Cesium before and after Irradiation

	Capacity of MAG*SEP^{SM} Particles, meq/g	
	Before Irradiation	Following Irradiation
Activated TVT MAG*SEP^{SM} Particles[a]	0.13	0.10
	0.12	0.10
	0.11	0.10
Resorcinol Formaldehyde MAG*SEP^{SM} Particles[a]	0.20	0.17
	0.19	0.16
	0.19	0.16
Silico-titanate MAG*SEP^{SM} Particles[b]	0.15	0.11
	0.16	0.13
	0.16	-
Clinoptilolite MAG*SEP^{SM} Particles[a]	0.17	0.11
	0.17	0.12
	0.17	0.11

[a]Particles received a dose of 6.4 Mrad.
[b]Particles received a dose of 9.7 Mrad.

From the testing performed to this point, silico-titanate MAG*SEP^{SM} particles were identified as being the most promising material to treat the Hanford supernatant. The irradiated particles, after exposure to a gamma dose equivalent to 100 cycles, were retested with the supernatant at its original concentration and at one-fifth the original concentration. The minimum particle-to-solution ratio was used for this study, i.e., 0.005 g of MAG*SEP^{SM} particles per milliliter of solution. In Table VI-4, the distribution ratios from this test are compared with the ratios obtained using nonirradiated silico-titanate MAG*SEP^{SM} particles (previously reported in Table VI-2.)

The results presented in Table IV-4 demonstrate a significant reduction in the K_d from the gamma exposure under both conditions tested. Since previous testing at Sandia National Laboratories had shown no degradation in the performance of crystalline silico-titanate after exposure to 10^9 rad using a Co-60 source, the observed decrease is most likely due to degradation of the organic matrix of the MAG*SEP^{SM} particles and not the adsorber materials themselves.

Table IV-4. Distribution Ratios for Non-irradiated and Irradiated Silico-titanate MAG*SEP^{SM} Particles

	Non-Irradiated Particles	Irradiated Particles[a]
Supernatant at the original concentration	102 108	22 28
Supernatant at one-fifth of the original concentration	353 685 369	151 130 —

[a]The particles received a dose of 9.7 Mrad.

A light microscopy study was undertaken to examine any effect on the MAG*SEP^{SM} particles as a consequence of gamma irradiation. The photographs showed the presence of particles much smaller than 100 μm and also the presence of fibrous material (refer to Part Two of the report). The observed effects may be attributed to the high OH^- concentration in the simulant waste stream present during irradiation, which caused the matrix of the MAG*SEP^{SM} particles to "unravel."

As a consequence of the effects observed in this study, modification and optimization of the methodology used to prepare the particles will be undertaken to provide more durable MAG*SEP^{SM} particles.

V. GENERAL DISCUSSION

The MAG*SEP^{SM} particles are of two types:

1. A basic core containing an outer surface with a functionalized chemical group.
2. A basic core that has smaller particles of a pre-existing ion exchanger attached to the surface.

The production of particles is often complicated by the materials to be used. Although a functional group or an ion exchange resin may be identified, it is not necessarily a straightforward process to attach these to a magnetic core.

The particles produced for this testing were prepared in a very short period and can only be considered prototypes. Optimization of particle preparation by Bradtec has shown improvements in both the mechanical properties and the ion exchange capacity. It is expected that further work would achieve similar results for any one of the particles used in this work.

In the case of the resorcinol resin, both types of particles (1 and 2 above) were produced. The resin produced at the Savannah River Site (SRS) was incorporated as small particles on a magnetic core. A second particle was produced in which the resorcinol grouping was prepared at Bradtec as a functionalized surface on the magnetic particle. Both these particles, as well as the unaltered resin from SRS, were tested for cesium capacity in a solution with no competing ions. The results indicated no differences between the three forms, and so the particles coated with the SRS resin were chosen to use in the test matrix.

It may, at first, appear surprising that a magnetic particle with a coating can have the same capacity as a resin bead. However, it is important to examine the circumstances of the test. The test is conducted to mimic the batch equilibrium which takes place within a very short time. In effect, it is unlikely that the resin and solution have come to equilibrium in such a short period. This results in only the counter ions in the outer layer of the resin bead and particles being exchanged. As this volume of resin is the same for both the particle and the bead, the capacities are equivalent under these test conditions.

For example, the capacity of a typical cation exchange resin is between 1.8 and 2.0 meq per gram of resin. Since the MAG*SEP^{SM} particles contain approximately 30% adsorber material, this equates to a capacity of 0.6 meq per gram of MAG*SEP^{SM} particles. If, as is the case, the adsorber material is embedded in a binding material on the MAG*SEP^{SM} particle, thus losing approximately one-third of its surface area to the binding material, the capacity is reduced still further, to approximately 0.4 meq per gram. The contact time used in this program of work was 15 min. This time is significantly shorter than is normally used to obtain a distribution ratio, where 12 to 72 h is more typical. Consequently, the term "distribution ratio" does not correctly describe the results obtained from this study. It may be more correct to consider them as a kinetic rate measurement. The values quoted in Table IV-3 show that the capacities of the MAG*SEP^{SM} particles incorporating the specific adsorber materials studied are comparable with the values that might be expected if a conventional cation exchange resin in the same conditions as described in this report was used to prepare the MAG*SEP^{SM} particles.

The K_ds resulting from these tests should be interpreted carefully. The K_d reported is for the resin type when associated with a magnetic core. As the calculation of the K_d involves the

concentration of cesium on the mass of beads, any inert material associated with the resin will tend to decrease the K_d in comparison with pure resin. In addition, production of the resin/bead particle is such that the beads are produced in a wet form. To avoid swelling stresses with untested beads, the particles are used wet, and the weights of particles recorded refer to the wet weight. The calculation of the K_d using the wet weight decreases the value. To summarize, the K_d for each resin type quoted in Table IV-3 is much lower than reported in the literature or would be determined in a test where the pure resin is used and allowed to come fully to equilibrium with the test solution.

Where MAG*SEP^{SM} technology offers a clear advantage over conventional ion exchange is during the handling of the process stream. The sediment in the bottom of the Hanford tank is composed of very small particles and will be disturbed easily on movement. Hence, it is likely that the supernatant will contain colloidal material and very fine particulate. If conventional ion exchange technology is used to treat this type of waste stream, the resin columns will become blocked very quickly and require frequent back-washing. However, MAG*SEP^{SM} particles can be added to a solution containing particulate and can be removed easily from the solution by using commercially available magnetic recovery systems.

Other important process advantages include a reduction in shielding requirements and residence time and, hence, a reduction of the exposure of the ion exchange resin to the gamma flux. The former problem of shielding is much reduced in the case of MAG*SEP^{SM}, as the process uses only a small quantity of resin at any one time, which is quickly regenerated and reused. The cesium waste can then be treated and stored appropriately. Conventional columns with large amounts of resin become extremely active as they operate and need heavy and costly shielding. Similarly, when used in a continuous short cycle, the ion exchanger is only exposed to the cesium gamma flux for short periods, unlike a column exchanger which is resident in the column for the whole loading cycle.

Regenerative solutions such as ammonia carbonate can be used to good effect with the MAG*SEP^{SM} approach. This solution can be evaporated to concentrate the cesium and condensed for reuse. The concentrated cesium can then be loaded onto an inorganic zeolite, which has good properties for cesium retention and radiation stability and is easily made into a glass for disposal.

VI. CONCLUSIONS

- The adsorbents were contacted with the Hanford supernate simulant for 15 min, which is consistent with the needs of the MAG*SEP^{SM} process. Longer contact times may produce higher K_d values (equilibrated).

- The MAG*SEP^{SM} particles coated with crystalline silico-titanate achieved the highest K_d values for cesium removal from the Hanford tank simulant under the conditions tested. The MAG*SEP^{SM} particles coated with resorcinol formaldehyde had the second highest K_d values.

- For all materials tested, the highest K_d values were observed when the simulant was diluted by one-fifth.

- The K_d values of the powdered adsorbents were not reduced by their incorporation into MAG*SEP^{SM} particles.

- The MAG*SEP^{SM} process offers clear advantages over conventional ion-exchange technology in terms of the method of application and handling. The rapid adsorption kinetics enables the particles to be added and removed from a process flowstream, and the magnetic filtration removes the concern of a secondary waste stream if suspended solids are present.

- The results presented in this report demonstrate the viability of using MAG*SEP^{SM} to remove cesium from Hanford tank supernatant. Future work should be performed to further refine the particle manufacture and the appropriate application conditions. This information should be used to develop an economic comparison between MAG*SEP^{SM} and conventional ion exchange.

APPENDIX A.

STATEMENT OF WORK AND METHODOLOGY

Background

The objective of this task is to optimize Bradtec's magnetic separation technology for cesium removal from Hanford tank supernatant. The supernatant is located in underground storage tanks at the Hanford site and contains radioactive Cs and Sr, and in some cases, low concentrations of transuranics.

Various MAG*SEP^{SM} particle coatings will be tested for their selective removal of cesium from Hanford tank supernatant simulant.

Scope of Work

Because actual supernatant is not available, a solution will be manufactured to simulate an average composition of the Hanford tanks. Four materials have been identified as possible candidates for cesium removal and have been prepared as MAG*SEP^{SM} particles (106 μm < particle size < 420 μm):

1. Activated TVT MAG*SEP^{SM}
2. Clinoptilolite MAG*SEP^{SM}
3. Resorcinol formaldehyde MAG*SEP^{SM}
4. Silico-titanate MAG*SEP^{SM}

The particles will then be tested to determine their ability to adsorb cesium while varying the following:

1. Ionic strength of the solution
2. Cesium concentration
3. Solution pH
4. MAG*SEP^{TM} particle-to-solution ratio

Work to Be Performed

The candidate adsorber materials will be tested, in powder form, for selective removal of cesium from Hanford tank supernatant simulant by measuring the distribution ratio (K_d = [Cs-137] adsorbent per gram/[Cs-137] treated solution per mL) between aqueous solution and adsorber materials. MAG*SEP^{SM} particles containing these adsorber materials will be prepared and tested while varying the parameters (1 through 4) above. In addition, the capacity of the MAG*SEP^{SM} particles will be determined with a solution containing no competing ions ("baseline" conditions). The capacity of the particles will be compared before and after irradiation with a gamma ray flux. Once the optimum type of MAG*SEP^{SM} particle and the best conditions have been identified, the K_d for the particles under these conditions will be compared before and after irradiation with a gamma ray flux.

The composition of the simulated tank supernatant is given in Table A-1 and the test matrix in Table A-2.

Table A-1. Recipe for Hanford Simulant Waste Stream

Major Components	Component Charge	Concentration, mol/L
Na	1	8.83
K	1	9.35×10^{-2}
Cs	1	4.88×10^{-5}
OH	-1	6.54
NO_3	-1	1.09
NO_2	-1	8.09×10^{-1}
$Al(OH)_4$	-1	2.06×10^{-2}
CO_3	-2	2.22×10^{-1}
CrO_4	-2	4.37×10^{-3}
PO_4	-3	8.00×10^{-4}

Table A-2. Matrix for MACS Testing

Experimental Variable	Maximum	Minimum
Two ionic strengths	Composition as Table A-1	Dilution by water to 1/5 of the above composition
Two Cs^+ concentrations	Composition as Table A-1	1/10 of the above composition
Two OH^- concentrations	Composition as Table A-1	Approx. 1M with $[Na^+]$ kept constant using $NaNO_3$ and $NaNO_2$ in their molar ratio given in Table A-1
Two adsorbent/solution ratios	0.05 g/mL[a]	0.005 g/mL[a]

[a]Particle-to-solution ratio.

Methodology

A. Preliminary Experiment to Identify Most Promising Adsorbent

Tests are to be performed on the following types of adsorbent:

- Powdered TVT
- Clinoptilolite (75 μm< particle size <180 μm)
- Clinoptilolite (45 μm< particle size <75 μm)
- Clinoptilolite (45 μm< particle size)
- Resorcinol formaldehyde

The preliminary tests involved the following steps:

1. Prepare the Hanford simulant waste solution according to Table A-1 as follows. Prepare 500 mL of simulant waste solution containing the following but do not make up to the mark of the volumetric flask.

   0.222M sodium carbonate (Na_2CO_3)

   0.00437M potassium chromate (K_2CrO_4)

   8.00 x 10^{-4}M dipotassium phosphate (K_2HPO_4)

   0.0206M aluminum hydroxide ($Al(OH)_3 \cdot H_2O$)

   0.0832M potassium chloride (KCl)

   6.54M sodium hydroxide (NaOH)

   1.09M sodium nitrate ($NaNO_3$)

   0.809M sodium nitrite ($NaNO_2$)

   4.88 x 10^{-5}M cesium chloride (CsBr)

   Total Na^+ burden = 0.444 + 6.54 + 1.09 + 0.809 = 8.883M
   Total K^+ burden = 0.00874 + 0.0016 + 0.0832 = 0.09354M

   Note: If all the salts do not dissolve, the solution will require filtering prior to spiking with Cs-137.

2. Add 5 kBq (135 nCi) Cs-137 to the solution and then make up to 500 mL. This will provide a solution containing 10 Bq/mL (270 pCi/mL) Cs-137. Store this solution in a plastic bottle.

3. Accurately weigh duplicate aliquots of approximately 1 g of each of the four types of adsorbent into a screw-top plastic Erlenmeyer flask. Record the weights in QA book.

4. Measure 20 mL of the Cs-137 spiked simulant solution into each flask and stir for 15 min. Record the actual contact time for each solution in QA book.

5. Decant each solution and filter the solution through a 0.2 μm glass microfiber filter.

6. Prepare duplicate 20 mL aliquots of the original Cs-137 spiked simulant solution.

7. Count the solutions plus one blank (deionized water) on a gamma spectrometer for 2000 s.

8. Determine the K_d for each type of MAG*SEP^{SM} particle according to the following equation: K_d = [Cs-137] adsorbent per gram/[Cs-137] treated solution per mL, where [Cs-137] adsorbent = [Cs-137] original solution minus [Cs-137] final solution.

B. Test Matrix

Do triplicate tests **only** if there are sufficient particles; otherwise do duplicates. If insufficient particles are available to perform tests using both weights of particles, use only the 0.005 g/mL test.

Ionic Strength as Given in Table A-1

1. Prepare 500 mL of simulant waste solution containing the following but do not make up to the mark.

   0.222M sodium carbonate (Na_2CO_3)

   0.00437M potassium chromate (K_2CrO_4)

   8.00×10^{-4}M dipotassium phosphate (K_2HPO_4)

   0.020M aluminum hydroxide [$Al(OH)_3 \cdot H_2O$]

   0.0832M potassium chloride (KCl)

   6.54M sodium hydroxide (NaOH)

   1.09M sodium nitrate ($NaNO_3$)

   0.809M sodium nitrite ($NaNO_2$)

   4.88×10^{-5}M cesium chloride (CsBr)

   Total Na^+ burden = 0.444 + 6.54 + 1.09 + 0.809 = 8.883M
   Total K^+ burden = 0.00874 + 0.0016 + 0.0832 = 0.09354M

   Note: If all the salts do not dissolve, the solution will require filtering prior to spiking with Cs-137.

2. Add 5 kBq (135 nCi) Cs-137 to the solution and then make up to 500 mL. This will provide a solution containing 10 Bq/mL (270 pCi/mL) Cs-137. Store this solution in a plastic bottle.

3. Where sufficient particles are available, weigh duplicate 1 g aliquots of each of the following types of MAG*SEP^{SM} particles into screw-top plastic Erlenmeyer flasks (record the weight in QA book). If insufficient particles are available, weigh triplicate 0.1 g aliquots of the particles.

   i. Activated TVT MAG*SEP^{SM} particles (106 μm < particle size < 420 μm)

   ii. Clinoptilolite MAG*SEP^{SM} particles (106 μm < particle size < 420 μm)

   iii. Resorcinol formaldehyde MAG*SEP^{SM} particles (106 μm < particle size < 420 μm)

   iv. Silico-titanate MAG*SEP^{SM} particles (106 μm < particle size < 420 μm)

4. Measure 20 mL of the simulant waste solution containing the Cs-137 into each of the flasks containing the MAG*SEP^{SM} particles and stir for 15 min.

5. Separate the particles from the solution using a magnet and filter through a 0.2 μm glass microfiber filter. Retain this solution for analysis in a plastic bottle.

6. Set up the gamma spectrometer and measure the peak area for a 20 mL aliquot of the simulant waste solution before contact with the MAG*SEP^{SM} particles. Count for 2000 s. Do this measurement on two separate 20 mL aliquots of the simulant waste solution.

7. Measure each of the solutions from step 5 for 2000 s to complete the mass balance for Cs-137.

8. Compare the counts obtained for the simulant waste solution before and after exposure to the MAG*SEP^{SM} particles and calculate the distribution ratio (K_d) for each of the particle types for Cs-137.

Ionic Strength One-fifth the Composition Given in Table A-1

1. Prepare 500 mL simulant waste solution containing the following but do not make up to the mark on the volumetric flask.

   0.044M sodium carbonate (Na_2CO_3)

   8.74 x 10^{-4}M potassium chromate (K_2CrO_4)

   1.6 x 10^{-4}M dipotassium phosphate (K_2HPO_4)

   4.12 x 10^{-3}M aluminum hydroxide [$Al(OH)_3 \cdot H_2O$]

   0.0166M potassium chloride (KCl)

   1.308M sodium hydroxide (NaOH)

   0.218M sodium nitrate ($NaNO_3$)

   0.1618M sodium nitrite ($NaNO_2$)

   9.76 x 10^{-6}M cesium chloride (CsBr)

   Total Na^+ burden = 1.7766M
   Total K^+ burden = 0.0187M

   Note: If all the salts do not dissolve, the solution will require filtering prior to spiking with Cs-137.

2. Add 5 kBq (135 nCi) Cs-137 to the solution and then make up to 500 mL. This will provide a solution containing 10 Bq/mL (270 pCi/mL) Cs-137. Store this solution in a plastic bottle.

3. Weigh triplicate 0.1 g aliquots of each of the following types of MAG*SEP^{SM} particles into screw-top plastic Erlenmeyer flasks (record the accurate weight in QA book).

   i. Activated TVT MAG*SEP^{SM} particles (106 μm < particle size <420 μm)

   ii. Clinoptilolite MAG*SEP^{SM} particles (106 μm < particle size <420 μm)

iii. Resorcinol formaldehyde MAG*SEP^{SM} particles (106 μm < particle size <420 μm)

iv. Silico-titanate MAG*SEP^{SM} particles (106 μm < particle size <420 μm)

4. Measure 20 mL of the simulant waste solution containing the Cs-137 into each of the flasks containing the MAG*SEP^{SM} particles and stir for 15 min.

5. Separate the particles from the solution using a magnet and filter through a 0.2 μm glass microfiber filter. Retain this solution for analysis in a plastic bottle.

6. Set up the gamma spectrometer and measure the peak area for a 20 mL aliquot of the simulant waste solution before contact with the MAG*SEP^{SM} particles. Count for 2000 s. Do this measurement on two separate 20 mL aliquots of the simulant waste solution.

7. Measure each of the solutions from step 5 for 2000 s to complete the mass balance for Cs-137.

8. Compare the counts obtained for the simulant waste solution before and after exposure to the MAG*SEP^{SM} particles and calculate the distribution ratio (K_d) for each of the particle types for Cs-137.

Cesium Concentration One-Tenth of Composition in Table A-1

1. Prepare 500 mL simulant waste solution containing the following but do not make up to the mark on the volumetric flask.

   0.222M sodium carbonate (Na_2CO_3)

   0.00437M potassium chromate (K_2CrO_4)

   8.00 x 10^{-4}M dipotassium phosphate (K_2HPO_4)

   0.0206M aluminum hydroxide [$Al(OH)_3 \cdot H_2O$]

   0.0832M potassium chloride (KCl)

   6.54M sodium hydroxide (NaOH)

   1.09M sodium nitrate ($NaNO_3$)

   0.809M sodium nitrite ($NaNO_2$)

   4.88 x 10^{-6}M cesium chloride (CsBr)

   Note: If all the salts do not dissolve, the solution will require filtering prior to spiking with Cs-137.

   Repeat steps 2 through 8 as given above.

Hydroxide Concentration 1M with [Na^+] Kept Constant

1. Prepare 500 mL simulant waste solution containing the following but do not make up to the mark on the volumetric flask.

0.222M sodium carbonate (Na_2CO_3)

0.00437M potassium chromate (K_2CrO_4)

8.00 x 10^{-4}M dipotassium phosphate (K_2HPO_4)

0.0206M aluminum hydroxide [$Al(OH)_3 \cdot H_2O$]

0.0832M potassium chloride (KCl)

1.0M sodium hydroxide (NaOH)

4.25 M sodium nitrate ($NaNO_3$)

3.15 M sodium nitrite ($NaNO_2$)

4.88 x 10^{-5}M cesium chloride (CsBr)

Note: If all the salts do not dissolve, the solution will require filtering prior to spiking with Cs-137.

Repeat steps 2 through 8 as given above.

C. Capacity of MAG * SEP^{SM} Particles before and after Irradiation

Prepare a "baseline" solution containing only inert cesium and a Cs-137 tracer as follows:

1. Weigh 0.1065 g of cesium bromide in 500 mL of deionized water to provide a solution containing 1 mM cesium. Spike this solution with 5 kBq (1.35 x 10^{-7} Ci) of Cs-137 to provide 10 Bq per mL of solution.

2. Accurately weigh triplicate aliquots containing approximately 0.1 g of each of the following MAG*SEP^{SM} particles into screw-top plastic Erlenmeyer flasks (record the weight in QA book).

   i. Activated TVT MAG*SEP^{SM} particles (106 μm < particle size <420 μm)

   ii. Clinoptilolite MAG*SEP^{SM} particles (106 μm < particle size <420 μm)

   iii. Resorcinol formaldehyde MAG*SEP^{SM} particles (106 μm < particle size <420 μm)

   iv. Silico-titanate MAG*SEP^{SM} particles (106 μm < particle size <420 μm)

3. Measure 20 mL of the baseline solution containing the Cs-137 into each of the flasks containing the MAG*SEP^{TM} particles and stir for 15 min.

4. Separate the particles from the solution using a magnet and filter through a 0.2 μm glass microfiber filter. Retain this solution for analysis in a plastic bottle.

5. Set up the gamma spectrometer and measure the peak area for a 20 mL aliquot of the baseline solution containing the Cs-137 before contact with the MAG*SEP^{SM} particles. Count for 2000 s. Do this measurement on two separate 20 mL aliquots of the baseline solution.

6. Measure each of the solutions from step 5 for 2000 s to complete the mass balance for Cs-137.

7. Compare the counts obtained for the baseline solution before and after exposure to the MAG*SEP^{SM} particles and calculate the capacity for each of the particle types for Cs-137.

8. Send the particles for irradiation with a gamma flux to Argonne National Laboratory.

9. Repeat the testing as described in steps 1 through 8 on the MAG*SEP^{SM} particles which have received the highest dose of gamma irradiation.

10. Compare the capacities of the MAG*SEP^{SM} particles before and after irradiation.

D. Distribution Ratio (K_d) before and after Irradiation

1. Repeat the test matrix (as described earlier) using only the Hanford simulant waste at the original concentration and at one-fifth the original concentration, on duplicate aliquots of approximately 0.1 g of irradiated crystalline silico-titanate particles. Use the particles which have been irradiated with the highest gamma flux.

2. Calculate the K_d for the particles and compare with the K_d obtained for the particles prior to irradiation.

Collation of the Raw Data

Notes to accompany data spreadsheets (see Appendix B):

i. Samples p-tvt-1 to resorcinol-2 = tests using powdered adsorbents only (Table IV-1).

ii. Samples tvt-mag*sep-A1 to cl-mag*sep-D3 = test matrix using MAG*SEP^{SM} particles (Table IV-2).

iii. Samples tvt-mag*sep-E1 to cl-irr-mag*-E3 = capacity testing on nonirradiated and irradiated MAG*SEP^{SM} particles (Table IV-3).

iv. Samples st-mag*sep-A1 to st-irr-mag*-B2 = testing on nonirradiated and irradiated MAG*SEP^{SM} particles coated with crystalline silico-titanate (Table IV-4).

v. Column entitled "sample counts" = counts obtained for samples corrected for background.

vi. Column entitled "standard counts" = counts obtained for solutions of the simulant waste stream and baseline prior to testing and corrected for background. The data are the average of duplicate measurements.

vii. Column entitled "standard activity Bq/mL" = activity in solutions of the simulant waste stream and baseline prior to testing and is equal to the amount of standard Cs-137 used to spike the solutions.

viii. Description of the solutions (final two digits in sample ID):

A = simulant waste stream at the original composition.
B = simulant waste stream at one-fifth of the original composition.
C = simulant waste stream containing one-tenth of the cesium concentration; the remaining components are present in their original concentration.
D = simulant waste stream containing 1 molar hydroxide; the remaining components are present in their original concentration.
E = "baseline solution," containing only inert cesium and Cs-137.

ix. The final digit in the sample ID (1 to 3) is the number of tests performed under these conditions and, hence, the number of samples analyzed, i.e., A1 to A3 = test samples 1, 2, and 3 for condition A.

x. MAG*SEP^{SM} particle description:

tvt = transylvanian volcanic tuff
rf = resorcinol formaldehyde
st = crystalline silico-titanate
cl/clino = clinoptilolite
irr = irradiated particles

Calculation of K_d

The experimental program depended on the measurement of ^{137}Cs in solution before and after contact with the ion exchange beads. The K_d was determined from the following equation[4]:

$$K_d = \frac{\text{concentration of } Cs^{137} \text{ in the particles}}{\text{concentration of } Cs^{137} \text{ in solution}} \left(\frac{\text{Bq g}^{-1}}{\text{Bq mL}^{-1}} \right) \qquad \text{(A-1)}$$

where concentration of cesium on MAG*SEP^{SM} particles = becquerels of cesium in original solution minus becquerels of cesium remaining in treated solution, all divided by the weight of MAG*SEP^{SM} particles used in the test; and concentration of cesium remaining in solution = becquerels of cesium remaining in the treated solution divided by the milliliters of solution tested. This relationship is derived by mass balance arguments.

E. Statistical Evaluation of K_d

In calculating K_d, the following approach has been taken in assessing the uncertainty associated with the final result (from Ref. 5). The experimental K_d was calculated as:

$$\frac{\text{initial sol. activity - final sol. } \bullet \text{ sample volume}}{\text{weight of resin}} \Big/ \text{final sol. activity} \qquad \text{(A-2)}$$

The activity of the initial spiked sample was counted in the measurement geometry to act as a secondary standard.

The sample activity was counted twice, and the uncertainty associated with the mean count is given as:

$$\sigma_x = \sqrt{\frac{\overline{X}}{N}} \tag{A-3}$$

σ_x = standard deviation of $\overline{X}$

$\overline{X}$ = mean of independent counts

N = number of independent counts

The activity of the final solution was measured by a single count with uncertainty:

$$\sigma_\gamma = \sqrt{Y} \tag{A-4}$$

The activity was calculated as:

$$\text{activity Y} = \frac{\text{Y counts}}{\overline{X}\text{ counts}} \left(\text{activity of } \overline{X}\right) \tag{A-5}$$

APPENDIX B.

MAG*SEP^{SM} PARTICLE IRRADIATION REPORT
ARGONNE NATIONAL LABORATORY

The following irradiated materials were used for capacity and testing:

Vial ID		
	B-1	Clinoptilolite MAG*SEP^{SM} particles - dose 6.4 Mrad ± 15%
	B-3	Clinoptilolite MAG*SEP^{SM} particles - dose 6.4 Mrad ± 15%
	B-5	Activated TVT MAG*SEP^{SM} particles - dose 6.4 Mrad ± 15%
	B-6	Activated TVT MAG*SEP^{SM} particles - dose 6.4 Mrad ± 15%
	B-13	Resorcinol formaldehyde MAG*SEP^{SM} particles - dose 6.4 Mrad ± 15%
	B-14	Resorcinol formaldehyde MAG*SEP^{SM} particles - dose 6.4 Mrad ± 15%
	B-19	Silico-titanate MAG*SEP^{SM} particles - dose 9.7 Mrad ± 30%
	B-20	Silico-titanate MAG*SEP^{SM} particles - dose 9.7 Mrad ± 30%

The table that follows summarizes the data obtained from testing these samples.

MAGNETICALLY ASSISTED CHEMICAL SEPARATION DEVELOPMENT PROGRAM

Sample Identification	Sample Counts	Sample Assoc. 1s error +/-	Standard Activity Bq/mL	Standard Counts*	Two Ind. Measures Assoc 1s error +/-	Standard to Sample Ratio	Ratio Assoc. error +/-	Sample Activity Bq/mL	Sample Assoc. 1s error +/-	Particle Weight grams	Calculated Kd	Kd Assoc. 1s error+/-
p-tvt-1	393	19.82	10	516	16.06	0.76	0.05	7.62	0.39	1.023	6	1.35
p-tvt-2	385	19.62	10	516	16.06	0.75	0.05	7.46	0.37	1.000	7	1.39
clino-75-180-1	407	20.17	10	450	15.00	0.90	0.06	9.04	0.56	1.027	2	1 41
clino-75-180-2	428	20.69	10	450	15.00	0.95	0.06	9.51	0.61	1.053	1	1.39
clino-45-74-1	362	19.03	10	450	15.00	0.80	0.06	8.04	0.46	1.040	5	1.40
clino-45-74-2	378	19.44	10	450	15.00	0.84	0.06	8.40	0.49	1.012	4	1 43
clino <45 -1	388	19.70	10	450	15.00	0.86	0.06	8.62	0.52	1.032	3	1.40
clino <45 -2	426	20.64	10	450	15.00	0.95	0.06	9.47	0.61	1.036	1	1.41
resorcinal-1	212	14.56	10	450	15.00	0.47	0.04	4.71	0.18	1.005	22	2.15
resorcinal-2	251	15.84	10	450	15.00	0.56	0.04	5.58	0.25	1.026	15	1.77
tvt-mag*sep-A1	425	20.62	10	517	16.08	0.82	0.05	8.22	0.44	1.012	4	1.34
tvt-mag*sep-A2	465	21.56	10	517	16.08	0.90	0.06	8.99	0.52	1.019	2	1.33
tvt-mag*sep-B1	343	18.52	10	411	14.34	0.83	0.06	8.35	0.51	0.101	39	15.02
tvt-mag*sep-B2	370	19.24	10	411	14.34	0.90	0.06	9.00	0.58	0.102	22	14.94
tvt-mag*sep-B3	368	19.18	10	411	14.34	0.90	0.06	8.95	0.58	0.100	23	15.09
tvt-mag*sep-C1	400	20.00	10	394	14.04	1.02	0.07	10.15	0.73	0.101	-3	-15.95
tvt-mag*sep-C2	397	19.92	10	394	14.04	2.01	0.07	10.08	0.72	0.101	-1	-15.84
tvt-mag*sep-C3	356	18.87	10	394	14.04	0.90	0.07	9.04	0.60	0.101	21	15.35
tvt-mag*sep-D1	416	20.40	10	424	14.56	0.98	0.07	9.81	0.66	0.100	4	15.25
tvt-mag*sep-D2	393	19.82	10	424	14.56	0.93	0.06	9.27	0.60	0.100	16	14.97
tvt-mag*sep-D3	411	20.27	10	424	14.56	0.97	0.07	9.69	0.65	0.100	6	15.15
rf-mag*sep-A1	388	19.70	10	465	15.25	0.83	0.06	8.34	0.48	0.101	39	14.09
rf-mag*sep-A2	360	18.97	10	465	15.25	0.77	0.05	7.74	0.42	0.100	58	14.40
rf-mag*sep-A3	381	19.52	10	465	15.25	0.82	0.06	8.19	0.46	0.102	43	14.00
rf-mag*sep-B1	244	15.62	10	411	14.34	0.59	0.05	5.94	0.28	0.101	136	17.73
rf-mag*sep-B2	226	15.03	10	411	14.34	0.55	0.05	5.50	0.25	0.102	161	18.84
rf-mag*sep-B3	145	12.04	10	411	14.34	0.35	0.03	3.53	0.12	0.101	364	30.34
rf-mag*sep-C1	208	14.42	10	394	14.04	0.53	0.05	5.28	0.24	0.106	168	19 03

* - Value represents an average of daily measurements

MAGNETICALLY ASSISTED CHEMICAL SEPARATION DEVELOPMENT PROGRAM

Sample Identification	Sample Counts	Sample Assoc. 1s error +/-	Standard Activity Bq/mL	Standard Counts*	Two Ind. Measures Assoc 1s error +/-	Standard to Sample Ratio	Ratio Assoc. error +/-	Sample Activity Bq/mL	Sample Assoc. 1s error +/-	Particle Weight grams	Calculated Kd	Kd Assoc. 1s error+/-
rf-mag*sep-C2	296	17.20	10	394	14.04	0.75	0.06	7.51	0.43	0.101	65	15.58
rf-mag*sep-C3	398	19.95	10	394	14.04	1.01	0.07	10.10	0.73	0.100	-2	-15.97
rf-mag*sep-D1	414	20.35	10	424	14.56	0.98	0.07	9.76	0.66	0.104	5	14.66
rf-mag*sep-D2	398	19.95	10	424	14.56	0.94	0.07	9.39	0.61	0.102	13	14.74
rf-mag*sep-D3	398	19.95	10	424	14.56	0.94	0.07	9.39	0.61	0.103	13	14.61
st-mag*sep-A1	117	10.82	10	419	14.47	0.28	0.03	2.79	0.08	1.055	49	13.72
st-mag*sep-A2	99	9.95	10	419	14.47	0.24	0.03	2.36	0.06	1.013	64	14.65
st-mag*sep-A3	256	16.00	10	419	14.47	0.61	0.05	6.11	0.30	0.118	108	14.65
st-mag*sep-A4	262	16.19	10	419	14.47	0.63	0.05	6.25	0.31	0.118	102	14.46
st-mag*sep-B1	148	12.17	10	411	14.34	0.36	0.03	3.60	0.12	0.101	353	29.64
st-mag*sep-B2	91	9.54	10	411	14.34	0.22	0.03	2.21	0.06	0.103	685	49.63
st-mag*sep-B3	142	11.92	10	411	14.34	0.35	0.03	3.45	0.12	0.103	369	30.41
st-mag*sep-B4	10	3.16	10	423	14.54	0.02	0.01	0.24	0.00	1.007	820	50.24
st-mag*sep-B5	19	4.36	10	423	14.54	0.04	0.01	0.45	0.47	1.010	421	26.31
st-mag*sep-C1	310	17.61	10	394	14.04	0.79	0.06	7.87	0.39	0.103	53	15.09
st-mag*sep-C2	279	16.70	10	394	14.04	0.71	0.06	7.08	0.28	0.102	81	15.95
st-mag*sep-C3	227	15.07	10	394	14.04	0.58	0.05	5.76	0.28	0.105	141	17.89
st-mag*sep-D1	174	13.19	10	424	14.56	0.41	0.04	4.10	0.15	0.103	278	24.77
st-mag*sep-D2	162	12.73	10	424	14.56	0.38	0.04	3.82	0.13	0.101	320	27.37
st-mag*sep-D3	278	16.67	10	424	14.56	0.66	0.05	6.56	0.33	0.105	100	15.57
cl-mag*sep-A1	440	20.98	10	465	15.25	0.95	0.06	9.46	0.60	0.100	11	14.38
cl-mag*sep-A2	469	21.66	10	465	15.25	1.01	0.07	10.09	0.67	0.101	-2	-14.16
cl-mag*sep-A3	422	20.54	10	465	15.25	0.91	0.06	9.08	0.55	0.101	20	14.19
cl-mag*sep-B1	324	18.00	10	411	14.34	0.79	0.06	7.88	0.46	0.100	54	15.22
cl-mag*sep-B2	297	17.23	10	411	14.34	0.72	0.06	7.23	0.40	0.101	76	15.56
cl-mag*sep-B3	341	18.47	10	411	14.34	0.83	0.06	8.30	0.50	0.100	41	15.13
cl-mag*sep-C1	389	19.72	10	394	14.04	0.99	0.07	9.87	0.70	0.100	3	15.81
cl-mag*sep-C2	341	18.47	10	394	14.04	0.87	0.06	8.65	0.55	0.105	30	14.74

* - Value represents an average of daily measurements

MAGNETICALLY ASSISTED CHEMICAL SEPARATION DEVELOPMENT PROGRAM

Sample Identification	Sample Counts	Sample Assoc. 1s error +/-	Standard Activity Bq/mL	Standard Counts*	Two Ind. Measures Assoc 1s error +/-	Standard to Sample Ratio	Ratio Assoc. error +/-	Sample Activity Bq/mL	Sample Assoc. 1s error +/-	Particle Weight grams	Calculated Kd	Kd Assoc. 1s error+/-
cl-mag*sep-C3	251	15.84	10	394	14.04	0.64	0.05	6.37	0.33	0.100	113	17.20
cl-mag*sep-D1	282	16.79	10	424	14.56	0.67	0.05	6.65	0.34	0.101	100	16.03
cl-mag*sep-D2	306	17.49	10	424	14.56	0.72	0.05	7.22	0.39	0.105	73	14.70
cl-mag*sep-D3	318	17.83	10	424	14.56	0.75	0.06	7.50	0.42	0.105	63	14.50
tvt-mag*sep-E1	168	12.96	10	460	15.17	0.37	0.03	3.65	0.12	0.101	346	28.21
tvt-mag*sep-E2	178	13.34	10	460	15.17	0.39	0.03	3.87	0.13	0.101	314	26.36
tvt-mag*sep-E3	202	14.21	10	460	15.17	0.44	0.04	4.39	0.16	0.101	252	22.81
tvt-irr-mag*-E1	205	14.32	10	392	14.00	0.52	0.05	5.23	0.24	0.132	138	15.47
tvt-irr-mag*-E2	196	14.00	10	392	14.00	0.50	0.04	5.00	0.22	0.137	146	15.64
tvt-irr-mag*-E3	226	15.03	10	392	14.00	0.58	0.05	5.77	0.28	0.110	13	17.01
rf-mag*sep-E1	24	4.90	10	460	15.17	0.05	0.01	0.52	0.01	0.106	3441	213.54
rf-mag*sep-E2	30	5.48	10	460	15.17	0.07	0.01	0.65	0.01	0.101	2847	178.24
rf-mag*sep-E3	32	5.66	10	460	15.17	0.07	0.01	0.70	0.01	0.102	2635	165.48
rf-irr-mag*-E1	64	8.00	10	392	14.00	0.16	0.02	1.63	0.04	0.101	1019	70.59
rf-irr-mag*-E2	72	8.49	10	392	14.00	0.18	0.02	1.84	0.04	0.100	886	62.80
rf-irr-mag*-E3	72	8.49	10	392	14.00	0.18	0.02	1.84	0.04	0.100	887	62.86
st-mag*sep-E1	125	11.18	10	460	15.17	0.27	0.03	2.72	0.07	0.102	526	38.76
st-mag*sep-E2	85	9.22	10	460	15.17	0.18	0.02	1.85	0.04	0.105	838	57.19
st-mag*sep-E3	99	9.95	10	460	15.17	0.22	0.02	2.15	0.05	0.103	711	49.76
st-irr-mag*E1	174	13.19	10	392	14.00	0.44	0.04	4.44	0.18	0.112	224	21.64
st-irr-mag*E2	136	11.66	10	392	14.00	0.35	0.03	3.47	0.12	0.116	326	27.34
cl-mag*sep-E1	72	8.49	10	460	15.17	0.16	0.02	1.57	0.03	0.101	1065	71.12
cl-mag*sep-E2	68	8.25	10	460	15.17	0.15	0.02	1.48	0.03	0.101	1143	75.81
cl-mag*sep-E3	60	7.75	10	460	15.17	0.13	0.02	1.30	0.02	0.102	1311	85.87
cl-irr-mag*-E1	185	13.60	10	392	14.00	0.47	0.04	4.72	0.20	0.124	181	18.33
cl-irr-mag*-E2	159	12.61	10	392	14.00	0.41	0.04	4.06	0.15	0.128	229	20.82
cl-irr-mag*-E3	185	13.60	10	392	14.00	0.47	0.04	4.72	0.20	0.101	221	22.43
st-mag*sep-A1	256	16.00	10	419	14.47	0.61	0.05	6.11	0.30	0.118	108	14.65

* - Value represents an average of daily measurements

MAGNETICALLY ASSISTED CHEMICAL SEPARATION DEVELOPMENT PROGRAM

Sample Identification	Sample Counts	Sample Assoc. 1s error +/-	Standard Activity Bq/mL	Standard Counts*	Two Ind. Measures Assoc 1s error +/-	Standard to Sample Ratio	Ratio Assoc. error +/-	Sample Activity Bq/mL	Sample Assoc. 1s error +/-	Particle Weight grams	Calculated Kd	Kd Assoc. 1s error+/-
st-mag*sep-A2	262	16.19	10	419	14.47	0.63	0.05	6.25	0.31	0.118	102	14.46
st-irr-mag*-A1	361	19.00	10	419	14.47	0.86	0.06	8.62	0.53	0.117	28	12.81
st-irr-mag*-A2	372	19.29	10	419	14.47	0.89	0.06	8.88	0.56	0.115	22	13.08
st-mag*sep-B1	148	12.17	10	411	14.34	0.36	0.03	3.60	0.12	0.101	353	29.64
st-mag*sep-B2	91	9.54	10	411	14.34	0.22	0.03	2.21	0.06	0.103	685	49.63
st-mag*sep-B3	142	11.92	10	411	14.34	0.35	0.03	3.45	0.12	0.103	369	30.41
st-irr-mag*-B1	225	15.00	10	423	14.54	0.53	0.04	5.32	0.23	0.117	151	16.74
st-irr-mag*-B2	240	15.49	10	423	14.54	0.57	0.05	5.67	0.26	0.118	130	15.64

* - Value represents an average of daily measurements

APPENDIX C.

GAMMA-SPECTROMETER CALIBRATION

Apparatus: Canberra 7000 Series

Ge(Li) Spectrometer Systems

Detector Model: 7222 S/N 113

Cryostat Model: 7500 S/N 113

Preamplifier Model: 1408 C special S/N 1230

A certified Cs-137 standard is counted for a known period of time (normally 1 h). The data from the activity of the source and the counting time are then fed to an analysis software program (spectra-AT CISE 526). The calibration graph is then calculated by computer.

For each new experiment, two samples of the solution prior to contact with MAG*SEP^{SM} particles are counted. The volume of these samples must be the same as the volume of the treated solution samples. Also, the geometry of the samples must be exactly the same.

The gamma-spectrometer system was checked (in February 1992) using a mixture of certified radionuclide standards. The efficiency and accuracy of the apparatus were examined. The apparatus is more efficient at low energy levels. The efficiency for Cs-137 is very low, but the accuracy is very good for all the radionuclides, with Cs-137 being one of the most accurate radionuclides.

REFERENCES

1. D. Bradbury, G. R. Elder, P. M. Tucker, and M. J. Dunn, "Treatment of Heavy Metals and Radionuclides in Groundwater and Wastewater by Magnetic Separation," ER '92 Symposium, p. 439 (September 1992).

2. D. White, Personal Communication, Department of Chemical Engineering, Imperial College, London.

3. S. F. Marsh, Z. V. Svitra, and S. M. Bowen, *Distribution of 14 Elements on 60 Selected Absorbers from Two Simulant Solutions (Acid - Dissolved Sludge and Alkaline Supernate for Hanford HLW Tank 102 - SY)* , Los Alamos National Laboratory Report LA-12654 (October 1993).

4. F. Helfferich, *Ion Exchange*, McGraw-Hill, New York (1962).

5. G. F. Knoll, *Radiation Detection and Measurement*, 2nd Ed., John Wiley & Son, New York (1989).

6. J. C. Miller and J. N. Miller, *Statistics for Analytical Chemistry*, 3rd Ed., Prentice Hall, London (1993).

PART TWO.

STUDIES OF GAMMA IRRADIATION AND OPTICAL MICROSCOPY ON CESIUM REMOVAL PARTICLES

(L. Nuñez,* B. A. Buchholz,* M. Ziemer,* G. Dyrkacz,**
M. Kaminski,* and G. F. Vandegrift*)

I. INTRODUCTION

Coated magnetic particles prepared by Bradtec were contacted with simulated Hanford supernatant and irradiated with a gamma dose equivalent to 10 and 100 cycles of use. These irradiated particles were then returned to Bradtec and re-tested for their absorption characteristics. We also performed optical microscopy of the Bradtec particles before and after irradiation equivalent to 10 and 100 cycles of use. The results were provided to Bradtec (see Part One).

II. GAMMA IRRADIATION

A. Irradiation of Bradtec Particles

Coated magnetic particles prepared by Bradtec (absorber material composed of clinoptilolite, resorcinol formaldehyde, and crystalline silico-titanate) were irradiated with a gamma dose equivalent to 10 and 100 cycles of use. A safety review was submitted and accepted by the CMT Safety Review Committee; the samples were irradiated in the Co-60 hot cell in the ANL Chemistry Division (diagram and information on source in Appendix A). Approximately 0.5 g of each irradiated sample was sealed in quartz tubes with 1.5 mL of the simulated supernatant solution (Part One, Table I-1). Dose estimates were computed on the basis of the size of the particles, estimates of the likely time needed to complete an irradiation cycle, and the following assumptions:

1. Average path length of radiation in magnetic particles is 80 μm.
2. Average values for the atomic number, atomic mass, and density of the magnetic particles are 14, 28, and 2.7 g/cm^3, respectively.
3. Contact time per extraction is 2 h.

These factors yield estimated doses of 6.79 x 10^5 rad and 6.79 x 10^6 rad for 10 and 100 cycles of use, respectively (see Sec. II.B).

Table II-1 contains information on the actual dose absorbed by the magnetic particles in the experiments.

---

*Argonne National Laboratory, Chemical Technology Division.
**Argonne National Laboratory, Chemistry Division.

Table II-1. Dose to Bradtec-Provided Samples of Coated Magnetic Particles

Vial	Bradtec ID	Mass, g	Dose, Mrad	Comments
B-1	clinoptilolite	0.5961	6.4	Beads absorbed liquid prior to irradiation.
B-2	clinoptilolite	0.4917	0.56	
B-3	clinoptilolite	0.4686	6.4	
B-4	clinoptilolite	0.5217	0.56	
B-5	activated TVT	0.4976	6.4	Sample B-15 contained 2 mL of solution.
B-6	activated TVT	0.6163	6.4	
B-7	activated TVT	0.5548	0.55	
B-8	activated TVT	0.5133	0.55	
B-9	resorcinol-formaldehyde UK form[a]	0.5549	6.4	Solution changed color from yellow to deep
B-10	resorcinol-formaldehyde UK form	0.5316	6.4	red upon contact with beads. Samples B-9 to
B-11	resorcinol-formaldehyde UK form	0.4678	0.55	B-16 appeared to behave similarly.
B-12	resorcinol-formaldehyde UK form	0.5474	0.55	
B-13	resorcinol-formaldehyde US form[b]	0.5192	6.4	Beads floated on top of solution when sealed.
B-14	resorcinol-formaldehyde US form	0.5897	6.4	Beads absorbed liquid prior to irradiation.
B-15	resorcinol-formaldehyde US form	0.5900	0.56	
B-16	resorcinol-formaldehyde US form	0.4806	0.56	
B-17	crystalline silico-titanate	0.5354	0.55	Solution changes color from yellow to rust on
B-18	crystalline silico-titanate	0.4980	0.55	contact. Liquid adsorbed prior to irradiation.
B-19	crystalline silico-titanate	0.5236	9.7	Rotor failure during irradiation.
B-20	crystalline silico-titanate	0.5061	9.7	

[a]Prepared by Bradtec, Ltd. (UK).
[b]Prepared by Bradtec, Inc. (US).

The doses absorbed by samples have an uncertainty of ±10-15%. The irradiation of two crystalline silico-titanate samples has a larger uncertainty in the dose (approximately ± 30-35%) due to the failure of the mechanical rotors used to rotate the test tubes containing samples. Hence, the dose to samples B-19 and B-20 is given as 9.7 ± 3.2 Mrad. The irradiated samples were returned to Bradtec for analysis (Part One). All the samples swelled after contact with the simulant supernatant. Those samples that entirely absorbed the solution showed the greatest swelling.

B. Radiation Dose Calculations

In order to approximate a real gamma dose, it is necessary to determine the time required for a complete cycle of the magnetic separation process. This estimation will determine the time necessary for gamma irradiation studies. This section discusses the method used to calculate the dose absorbed by the cesium-specific magnetic particles from Bradtec.

The particles provided by Bradtec were 100-400 μm. Since the kinetic energy of the emitted ß-particles is deposited over a short range, the dose absorbed by large particles is significantly higher than that absorbed by smaller particles. The doses anticipated to be absorbed by the cesium-specific magnetic particles were calculated by considering the ß-particle and γ-ray

emitted by Cs-137. The ß-particles are expected to deposit much more energy per unit path length than do the γ-rays. The emitted ß-particle and a neutrino share 514 keV, producing an energy spectrum of emitted ß-particles. The most probable kinetic energy of the ß-particle is 1/3 E_{max}, or 171 keV. This energy is typically used when computing doses from ß-particles. Ionization of target atoms is the principal mechanism for energy deposition.

The energy deposited in the magnetic particles was determined by using an expression for the loss in kinetic energy per unit path length (Eq. II-1) and approximating the energy deposited by γ-rays using an attenuation coefficient (Eq. II-2).[1] The energy deposited by the ß-particle is given by

$$\frac{dE}{dX} = \frac{2\pi q^4 NZ(3x10^9)^4}{E_m\beta^2(1.6x10^{-6})^2}\left\{\ln\left[\frac{E_m E_k \beta^2}{I^2(1-\beta^2)}\right]-\beta^2\right\}\frac{MeV}{cm} \qquad \text{(II-1)}$$

where

q = charge of an electron = 1.6 x 10^{-19} C,

N = number of absorber atoms per cm^3,

Z = atomic number of absorber,

NZ = electron density of absorber, in electrons/cm^3

E_m = rest energy of a β-particle = 0.511 MeV,

E_k = kinetic energy of the β-particle, in eV

β = v/c (where v = velocity of β-particle, cm/s; and c = speed of light, cm/s)

I = mean ionization and excitation potential of absorber = Z • 13.5 eV.

The numerical factors in Eq. II-1 are used to produce convenient units (MeV/cm). The absorption and attenuation coefficients for the magnetic particles are approximately equal. Equation I-2 gives an expression for the intensity (I) of γ-rays having passed through an absorber of thickness x (cm) and absorption coefficient μ (cm^{-1}) compared to the initial intensity I_o:

$$I = I_o[1-\exp(-\mu x)] \qquad \text{(II-2)}$$

The ratio I/I_o gives the fraction of γ-rays absorbed when passing through the absorber. It was assumed that any γ-ray that interacted with the particles deposited all its energy. Since the magnetic particles are relatively transparent to 660 keV photons, the γ-rays deposited much less energy than did the ß-particles.

The electron density of the target must be determined to compute the absorbed dose. Since Bradtec was unable to provide detailed information regarding particle density, average atomic number, and average atomic mass, several values within a reasonable range were used to compute estimates.

The Bradtec particles were larger than expected, and since the dose absorbed depends on the path length of the ionizing radiation through the particle, they received a large dose. The assumptions used when calculating doses are as follows:

1. Half of the ß-particles are emitted into solution, resulting in no energy deposited to the magnetic particles.
2. Beta-particles interact with only one magnetic particle.
3. All γ-rays interact with magnetic particles.
4. The energy deposited by γ-rays depends solely on the attenuation of the ^{137}Cs gamma ray.
5. All cesium in the supernatant solution absorbed on particles.
6. One gram of particles was assumed per liter of solution.
7. The concentration of Cs-137 in the supernatant is 4.88×10^{-5} mol/L.

Using these assumptions and the equations above for energy deposition as a function of path length, the dose to the magnetic particles was estimated for different path lengths, atomic numbers, atomic masses, and densities, and the results are presented in Table II-2. The results were used as the basis for ^{60}Co gamma irradiation of the particles.

Table II-2. Calculated Dose Absorbed by Cesium-Specific Magnetic Particles

Path Length, μm	Target Z	Target A	Target Density, g/cm^3	Beta Energy,[a] MeV	Gamma Energy,[a] MeV	Contact Time, h	Dose, rad	
							10 Contacts	100 Contacts
20	12	24	2.5	6.26E+03	2.65E+02	0.5	4.02E+04	4.02E+05
40	12	24	2.5	1.25E+04	5.29E+02	0.5	8.04E+04	8.04E+05
60	12	24	2.5	1.88E+04	7.94E+02	0.5	1.21E+05	1.21E+06
80	12	24	2.5	2.51E+04	1.06E+03	0.5	1.61E+05	1.61E+06
100	12	24	2.5	3.13E+04	1.32E+03	0.5	2.01E+05	2.01E+06
20	14	28	2.7	6.62E+03	2.65E+02	0.5	4.24E+04	4.24E+05
40	14	28	2.7	1.32E+04	5.29E+02	0.5	8.48E+04	8.48E+05
60	14	28	2.7	1.99E+04	7.94E+02	0.5	1.27E+05	1.27E+06
80	14	28	2.7	2.65E+04	1.06E+03	0.5	1.70E+05	1.70E+06
100	14	28	2.7	3.31E+04	1.32E+03	0.5	2.12E+05	2.12E+06
20	12	24	2.5	6.26E+03	2.65E+02	1	8.04E+04	8.04E+05
40	12	24	2.5	1.25E+04	5.29E+02	1	1.61E+05	1.61E+06
60	12	24	2.5	1.88E+04	7.94E+02	1	2.41E+05	2.41E+06
80	12	24	2.5	2.51E+04	1.06E+03	1	3.22E+05	3.22E+06
100	12	24	2.5	3.13E+04	1.32E+03	1	4.02E+05	4.02E+06
20	14	28	2.7	6.62E+03	2.65E+02	1	8.48E+04	8.48E+05
40	14	28	2.7	1.32E+04	5.29E+02	1	1.70E+05	1.70E+06
60	14	28	2.7	1.99E+04	7.94E+02	1	2.54E+05	2.54E+06
80	14	28	2.7	2.65E+04	1.06E+03	1	3.39E+05	3.39E+06
100	14	28	2.7	3.31E+04	1.32E+03	1	4.24E+05	4.24E+06
20	12	24	2.5	6.26E+03	2.65E+02	2	1.61E+05	1.61E+06
40	12	24	2.5	1.25E+04	5.29E+02	2	3.22E+05	3.22E+06
60	12	24	2.5	1.88E+04	7.94E+02	2	4.83E+05	4.83E+06
80	12	24	2.5	2.51E+04	1.06E+03	2	6.44E+05	6.44E+06
100	12	24	2.5	3.13E+04	1.32E+03	2	8.04E+05	8.04E+06
20	14	28	2.7	6.62E+03	2.65E+02	2	1.70E+05	1.70E+06
40	14	28	2.7	1.32E+04	5.29E+02	2	3.39E+05	3.39E+06
60	14	28	2.7	1.99E+04	7.94E+02	2	5.09E+05	5.09E+06
80	14	28	2.7	2.65E+04	1.06E+03	2	6.79E+05	6.79E+06
100	14	28	2.7	3.31E+04	1.32E+03	2	8.48E+05	8.48E+06

[a]Deposit decay.

III. OPTICAL MICROSCOPY

A. Optical Microscopy before Irradiation

Upon contact of the Bradtec particles with the Hanford supernatant simulant, the liquid was completely absorbed by the particles, and in some cases, the solution color changed. The large size of these particles precluded them as candidates for transmission electron microscopy (TEM). However, we were able to observe the particles (before irradiation) under an optical microscope and determine general features and size distributions. Results are given below for the analyses of crystalline silico-titanate, resorcinol, clinoptilolite, and transylvanian volcanic tuff particles.

Photographs of all samples were taken using a light microscope. One micrograph was made for each of the samples, and an additional micrograph was taken and included a physical scale to be used in size determination. The pictures obtained were then digitized and analyzed by two different computer programs: National Institute of Health Image 1.49 and Ultimage/24 2.1. The digitized pictures were then enhanced. The first step was to physically white-out the background, leaving behind only the particle images. Next, the programs were used to find the maximum diameter of each particle. These results are present in the form of a histogram. Particle distributions are given in Figs. III-1 to III-4 and micrographs in Figs. III-5 to III-8.

The particles in the crystalline silico-titanate sample did not seem to align themselves with the induced magnetic field from the transformer of the microscope, as some of the others did. Most of the particles were smaller than 300 μm in diameter (Fig. III-1). The particles appeared to be original particles and not chips. The particles were round and did not appear to be fractured larger particles. This sample also contained a number of thread-like structures. The thread-like structures appeared to be fibers that had entered the sample during production. They could possibly be fibers from filters. (We looked at another sample after the microscope was cleaned and verified that the threads were in the sample, not on the lens or eyepiece of the microscope).

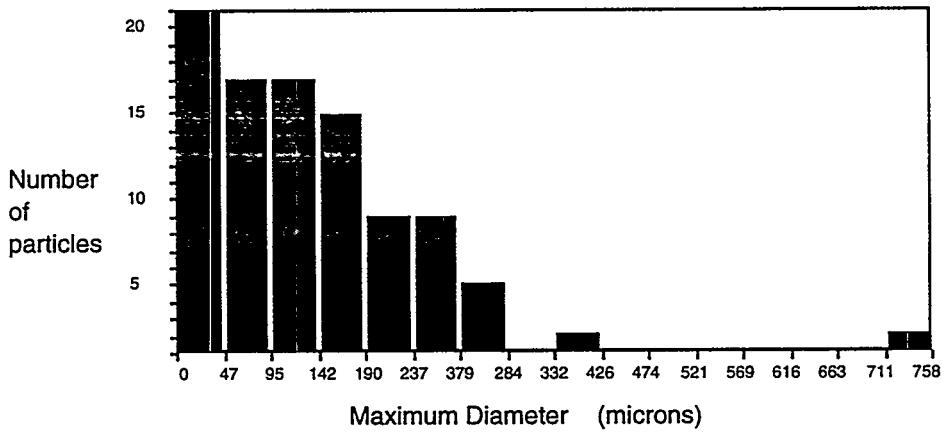

Fig. III-1. Particle Distribution of Crystalline Silico-Titanate Particles (number of particles, 90; mean diameter, 132.6 μm)

The resorcinol (US form) sample (Fig. III-2) was composed of a few particles over 500 μm and numerous others smaller than 100 μm. This sample also contained a number of thread-like structures.

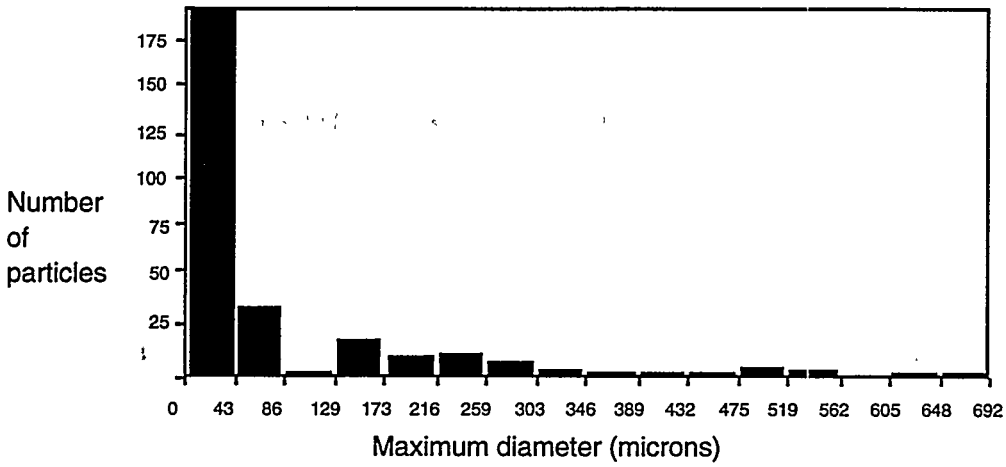

Fig. III-2. Particle Distribution of Resorcinol (US form) Particles (number of particles, 307; mean diameter, 83.8 μm)

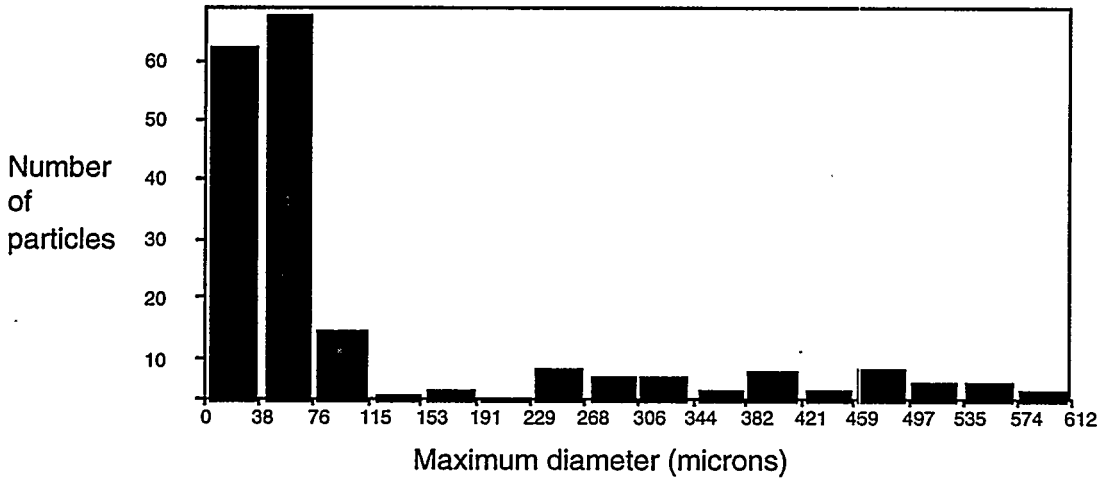

Fig. III-3. Particle Distribution of Resorcinol (UK form) Particles (number of particles, 189; mean diameter, 110.5 μm)

The resorcinol (UK form) sample (Fig. III-3) was composed of a number of particles with diameters greater than 300 μm, as well as numerous others with diameters less than 100 μm. Very few particles were found with diameters in the 100 to 300 μm range. The micrograph (Fig. III-7) suggests that there may be some attraction between the larger particles.

For the clinoptilolite sample (Fig. III-4), the magnetic particles aligned themselves with the magnetic field induced by the transformer used to provide the light for the microscope. This led to some inaccuracy in counting the particles. Analyzing the particles required that a white line be drawn between them. The smaller particles, in the 0 to 50 μm range, did not align themselves with the larger ones. This suggests that the smaller particles may not contain magnetite, or at least that the particles do not contain enough magnetite for the field produced by the transformer to have an effect, but this would not discern if small particles are in contact with larger particles.

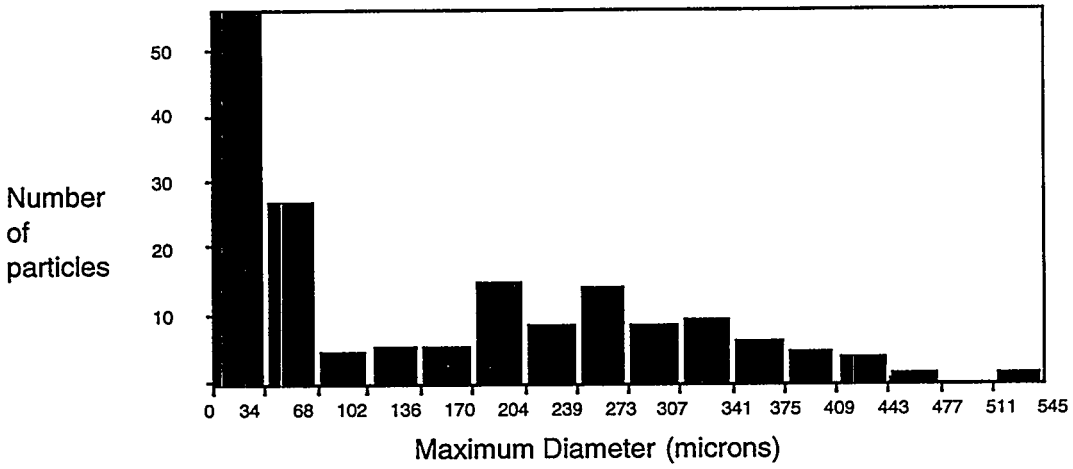

Fig. III-4. Particle Distribution of Clinoptilolite Particles
(number of particles, 185; mean diameter, 150.0 μm)

The particles of the activated transylvanian volcanic tuff samples were aligned in chains; however, the photograph was too dark to be analyzed using the software available (figures therefore not included). The particles appear to be in the 200 to 300 μm region. There are also a number of particles less than 50 μm in diameter scattered throughout the sample. This micrograph showed a large thread-like structure, perhaps composed of a few smaller strands.

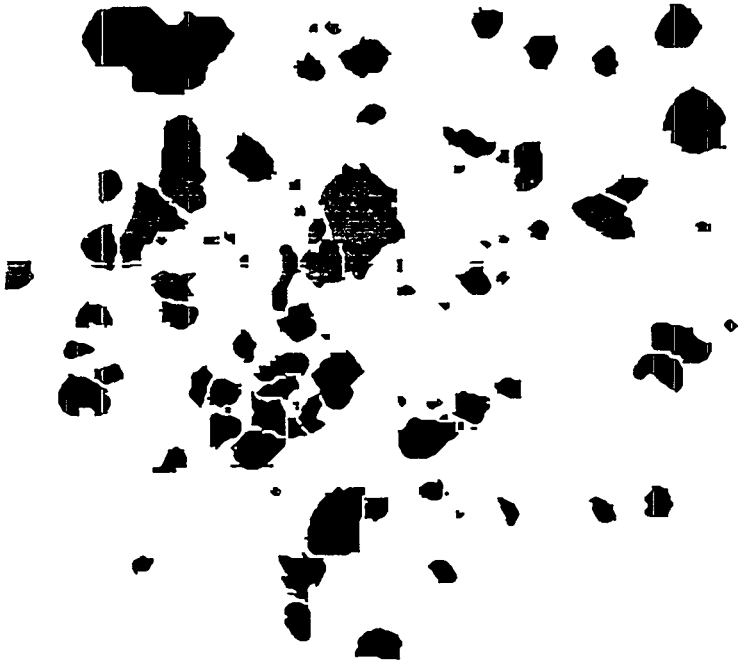

Fig. III-5. Micrograph of Crystalline Silico-Titanate Particles

Figures III-5 through III-8 show the micrographs obtained with the whited-out background and Ultimage/24 analysis. In Fig. III-5, the random alignment of the silico-titanate particles is apparent. The particles did not appear to be fragmentations from larger particles. Figure III-6 shows the prominence of fines in the presence of larger particles (> 500 μm) for the resorcinol

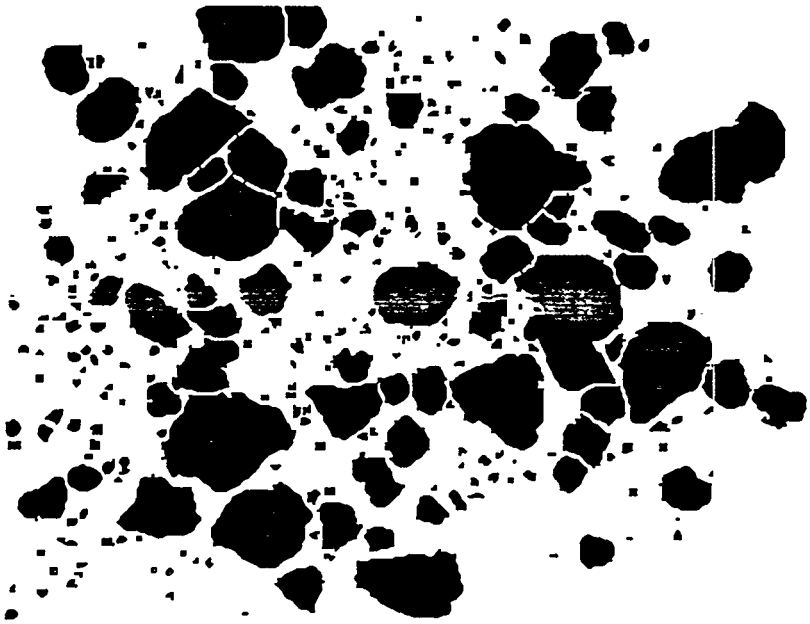

Fig. III-6. Micrograph of Resorcinol (US form) Particles

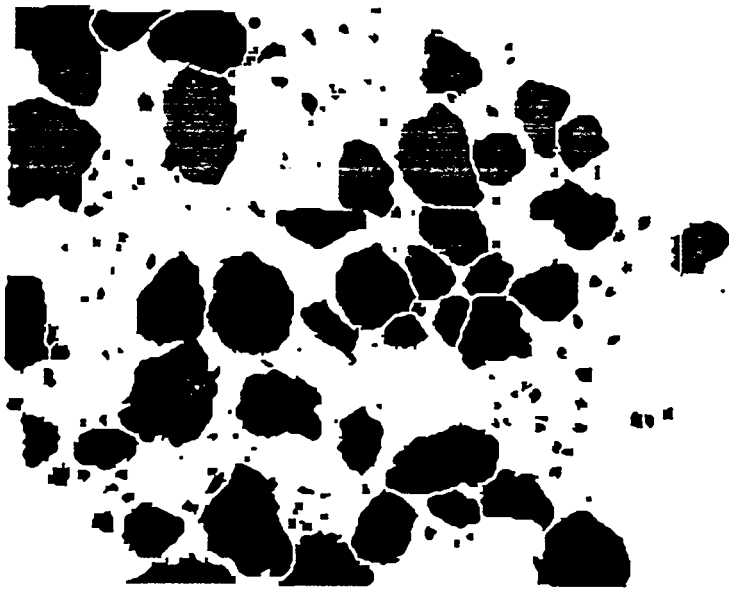

Fig. III-7. Micrograph of Resorcinol (UK form) Particles

(US form) sample. Figure III-7 shows the presence of a large number of particles smaller than 100 μm and larger than 300 μm in the resorcinol (UK form) sample. The alignment of the clinoptilolite particles with the induced magnetic field is well illustrated in Fig. III-8. The close-packing led to estimates on the position of the natural breaks between particles.

In general, the majority of the particles were smaller than 100 μm, with the largest ones being over 700 μm. All of the samples displayed a distribution between these two values. Standard deviations (not included in this report), which were much greater than the mean values in all cases, demonstrated the large variation in the particle sizes. The resolution at the magnification used was 13 μm. All of the photographs also showed the presence of tiny particles (less than 50 μm) scattered throughout the samples.

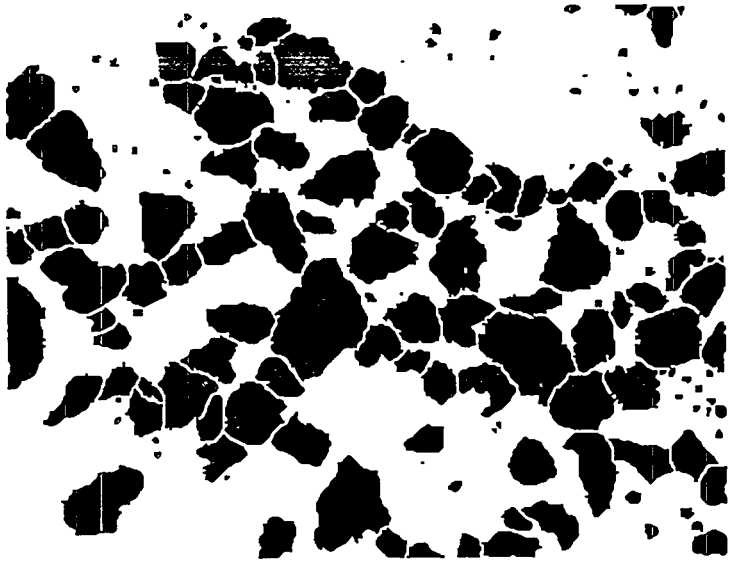

Fig. III-8. Micrograph of Clinoptilolite Particles

B. Optical Microscopy after Gamma Irradiation

Optical micrographs were taken to help determine the effect of radiation on two sets of particles provided by Bradtec: crystalline silico-titanate and resorcinol. The micrographs were taken with a Leitz light microscope at 32 times magnification. The images were then digitized with a Hewlett Packard scanner and Ofoto software. All of the micrographs were edited according to the procedure described in the previous section. The distribution of particles according to maximum diameter and total area is included along with each micrograph.

1. Crystalline Silico-Titanate Samples

Figure III-9 is the micrograph obtained before irradiation of crystalline silico-titanate contacted by supernatant. The particles did not appear to align themselves with a magnetic field, as did some of the other particle types. Most of the particles were smaller than 300 μm in diameter but probably still contained iron particles (Figs. III-10 and III-11). This sample also contained a number of thread-like structures of unknown origin. These were recognized as being of a different composition than the polymer that constitutes the silico-titanate particle core. We

looked at another sample after the microscope was cleaned and verified that the threads were in the sample, not on the lens or eyepiece of the microscope.

Fig. III-9. Micrograph of Crystalline Silico-titanate Particles before Irradiation

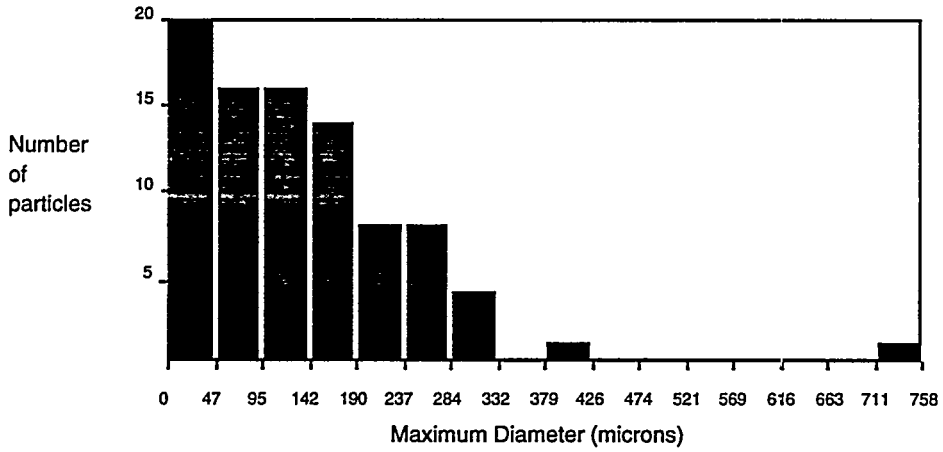

Fig. III-10. Distribution of Crystalline Silico-titanate Particles in Fig. III-9 as Function of Diameter (average value, 133 μm)

In Fig. III-12, the supernatant waste simulant has been added to the particles, and swelling has occurred. In the comparison between this micrograph and Fig. III-9, the average particle diameter increased by approximately 100 μm (Figs. III-13 and III-14). This sample also contained some material that appeared to be glass particles, which were bound to the silico-titanate resin and appear as fine particles in the figure. It was concluded that this material must be the

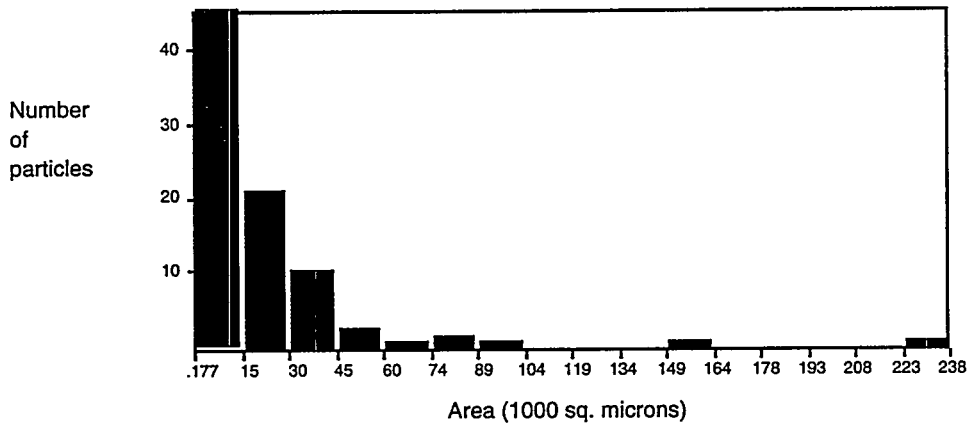

Fig. III-11. Distribution of Crystalline Silico-titanate Particles in Fig. III-9 as Function of Area (average value, 22,000 μm^2)

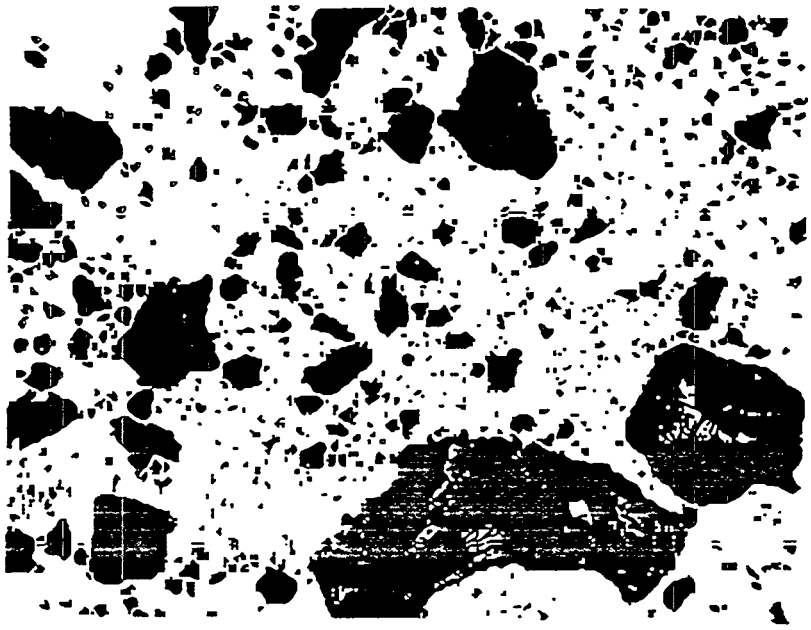

Fig. III-12. Micrograph of Swelled Silico-titanate before Irradiation

translucent polymer beneath the absorber material. Since the particles were exposed to the basic waste solution for a time comparable to 100 cycles (> 2 days), their degradation could have occurred, releasing the resin coating and exposing the polymer core. We would expect the extraction capabilities to be severely depressed as a result. In the samples that were irradiated, glass shards were present due to the sealed quartz vials having been opened. Moreover, the glass appears as colorless objects with sharp, jagged sides.

The micrographs of the silico-titanate sampled irradiated for the equivalent of 10 cycles (Fig. III-15) show the effect of radiation on the particles. The particles are starting to aggregate (Figs. III-16 and III-17), reducing the surface area of the particles available for contact with the waste to be extracted.

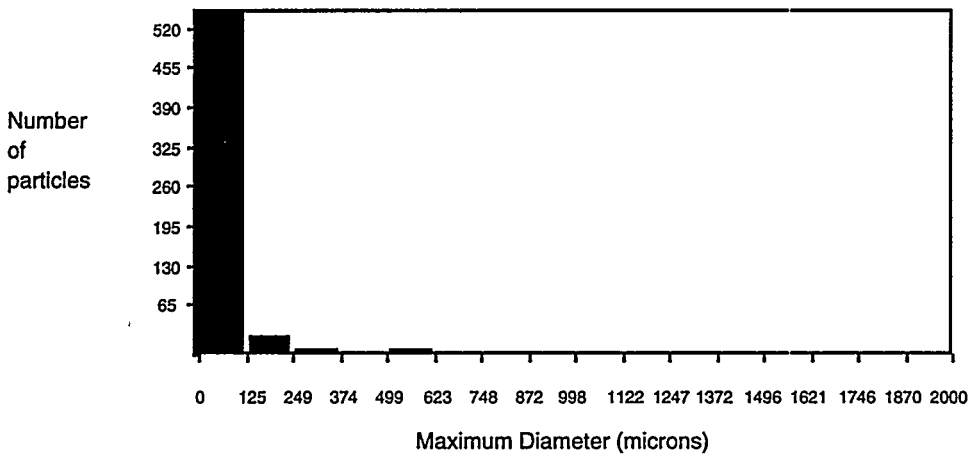

Fig. III-13. Particle Distribution for Silico-titanate Sample in Fig. III-12 as Function of Diameter (average value, 55 μm)

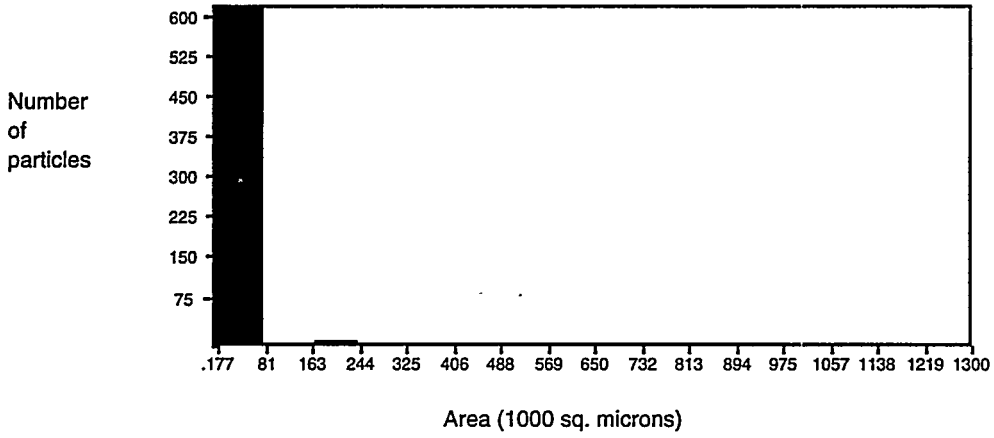

Fig. III-14. Particle Distribution for Silico-titanate Sample in Fig. III-12 as Function of Area (average value, 8200 μm^2)

The micrograph of the silico-titanate sample irradiated for 100 cycles (Fig. III-18) continues the trend that began with low radiation doses. The particles are forming larger aggregates, 1000 to 1200 μm in diameter. Once again, some glass was found in the sample but is not visible in the figures presented (Figs. III-19 and III-20). The tremendous decrease in surface area indicated by this micrograph provides a possible answer to the low K_d values recorded (see Part One), since it is the silico-titanate on the surface of the particles which complexes the waste.

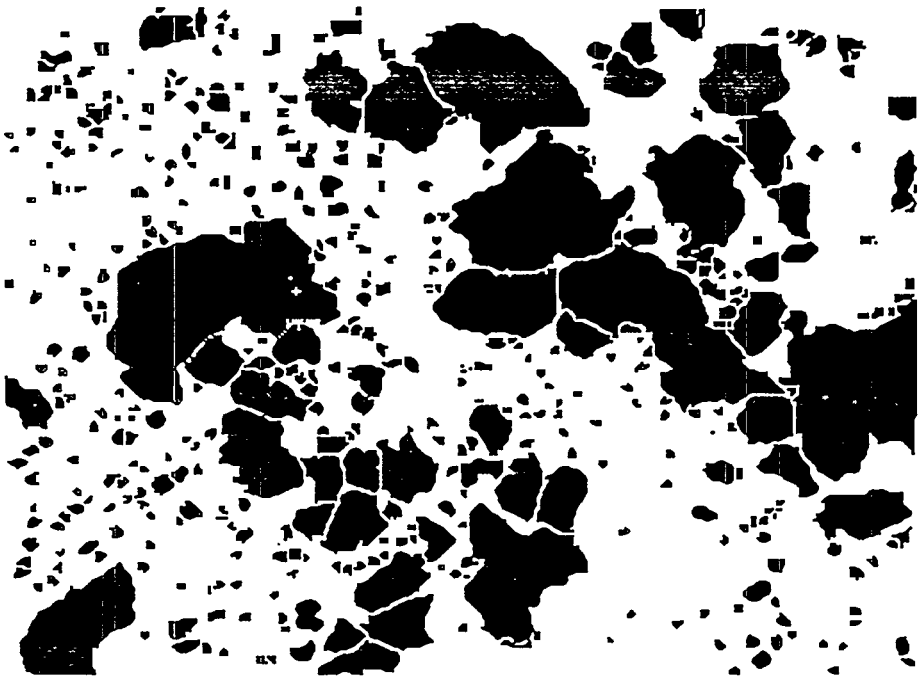

Fig. III-15. Micrograph of Silico-titanate Sample Irradiated for 10 Cycles

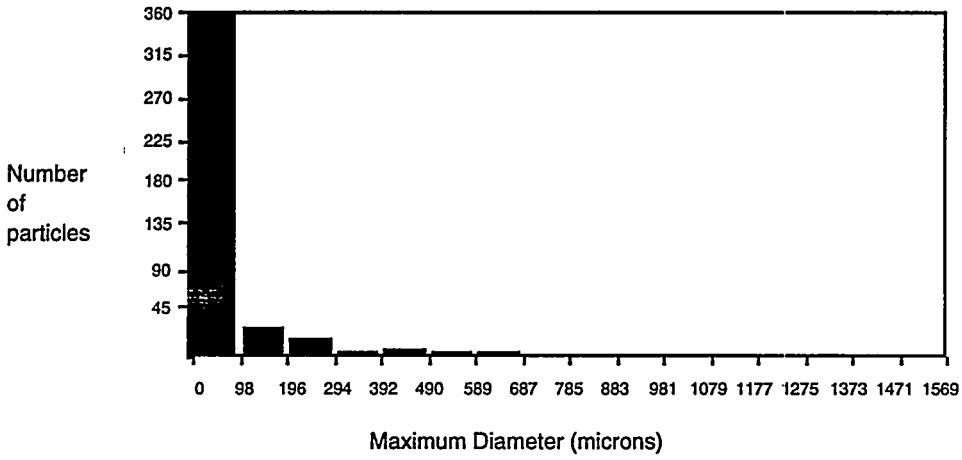

Fig. III-16. Particle Distribution for Silico-titanate Sample in Fig. III-15 as Function of Diameter (average value, 71 μm)

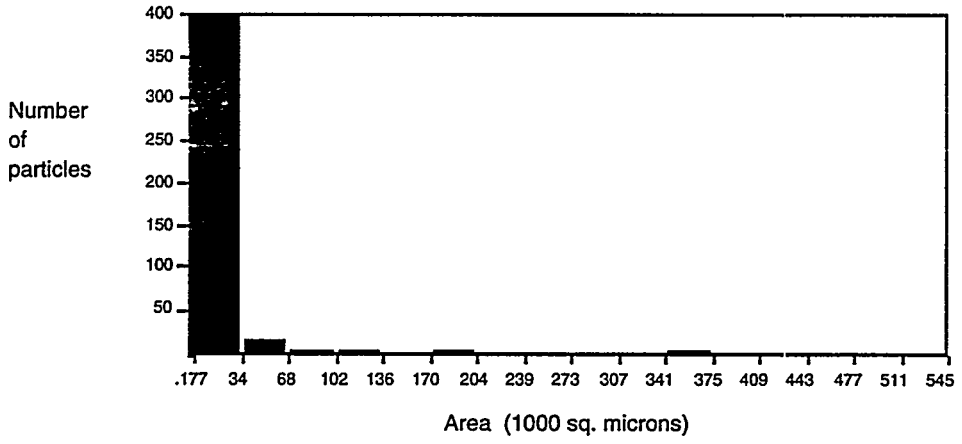

Fig. III-17. Particle Distribution for Silico-titanate Sample in Fig. III-15 as Function of Area (average value, 12,000 μm^2)

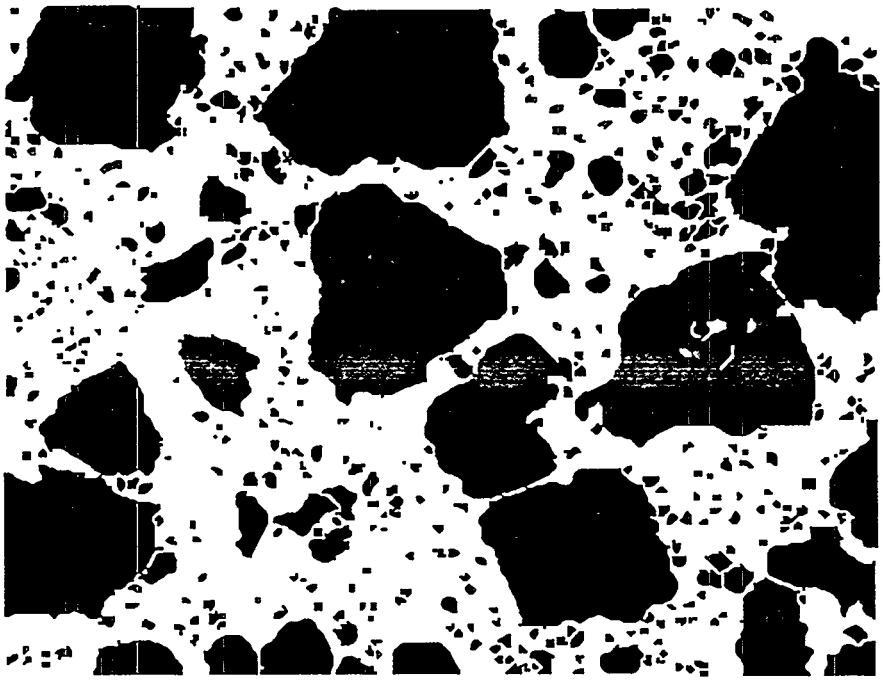

Fig. III-18. Micrograph of Silico-titanate Sample Irradiated for 100 Cycles

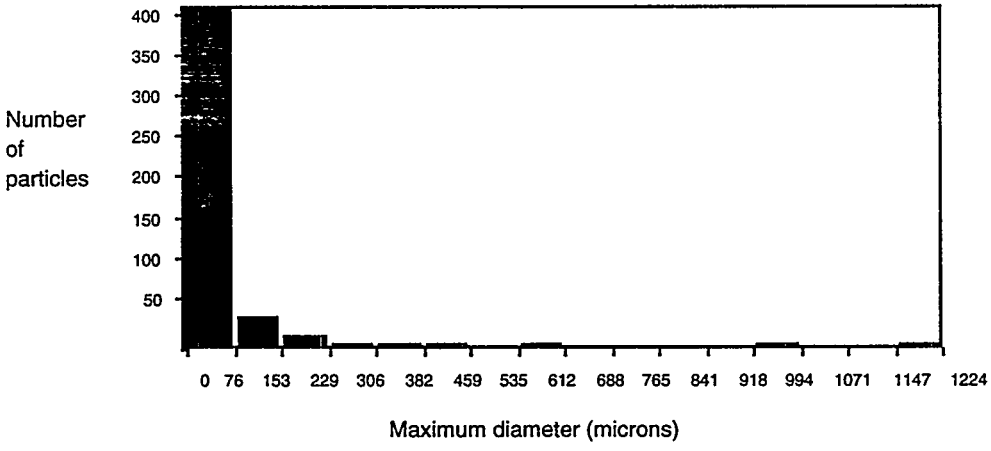

Fig. III-19. Particle Distribution of Silico-titanate Sample in Fig. III-18 as Function of Diameter (average value, 64 μm)

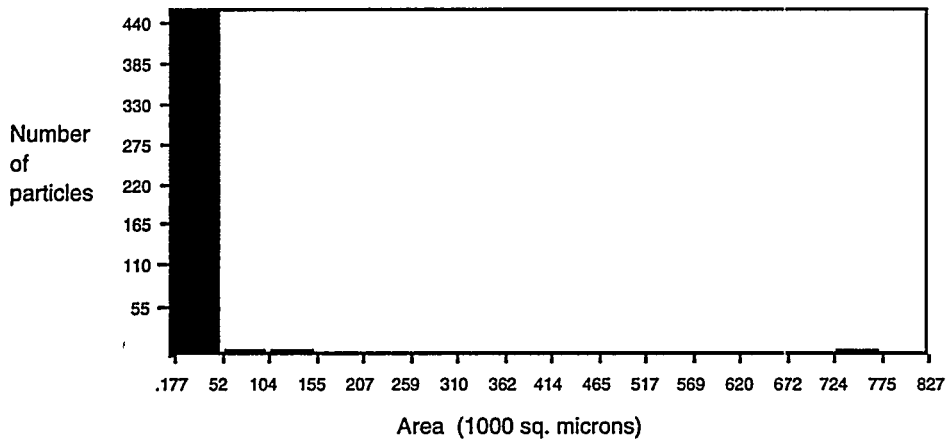

Fig. III-20. Particle Distribution of Silico-titanate Sample in Fig. III-18 as Function of Area (average value, 150,000 μm^2)

2. Resorcinol Particles (US Form)

The micrograph of a resorcinol sample irradiated for 100 cycles (Fig. III-21) was composed of a few particles over 500 μm and numerous others smaller than 100 μm (Figs. III-22 and III-23). This sample also contained a number of thread-like structures.

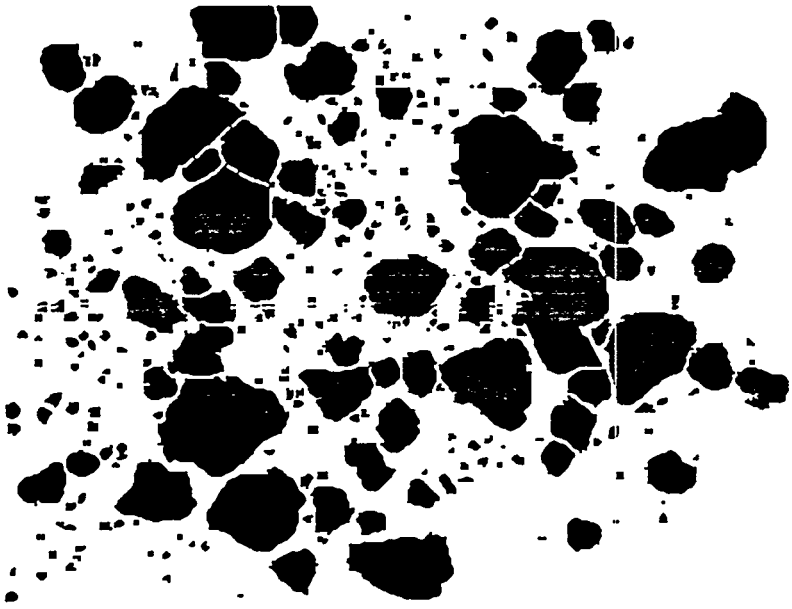

Fig. III-21. Micrograph of Resorcinol (US form) Sample before Irradiation

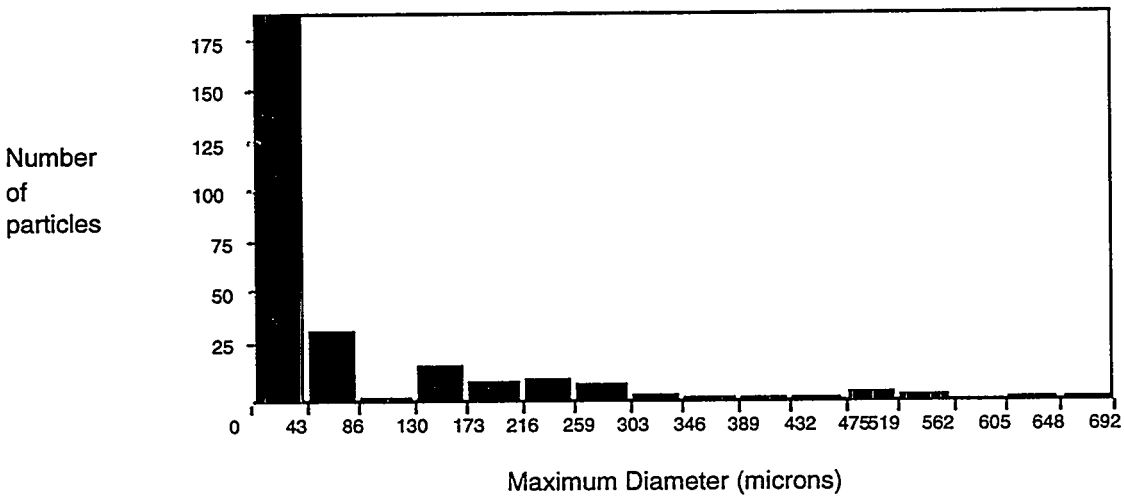

Fig. III-22. Particle Distribution of Resorcinol Sample in Fig. III-21 as Function of Diameter (average value, 84 μm)

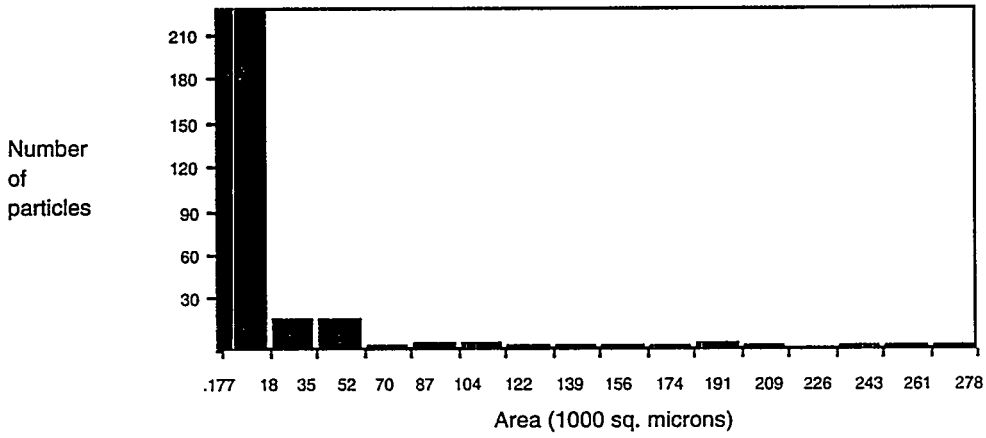

Fig. III-23. Particle Distribution of Resorcinol Sample in Fig. III-21 as Function of Area (average value, 16,000 μm^2)

In the micrograph (Fig. III-24) and particle distribution (Figs. III-25 and III-26), it appears that the particles have swelled. The sizes of the large particles are 100 to 200 μm greater than those of the previous micrograph (Fig. III-6). A possible explanation is that the polymer is absorbing the liquid. This is similar to the results that Bradtec obtained when trying to extract ^{137}Cs from milk, where the absorption of liquid into the particles produced milk enriched in calcium.

Fig. III-24. Micrograph of Swelled Resorcinol Sample (US form)

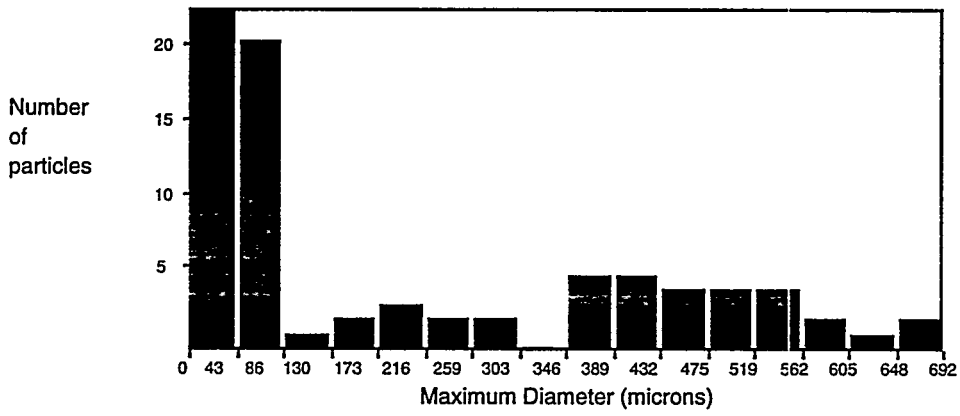

Fig. III-25. Particle Distribution of Resorcinol Sample in Fig. III-24 as Function of Diameter (average value, 197 μm)

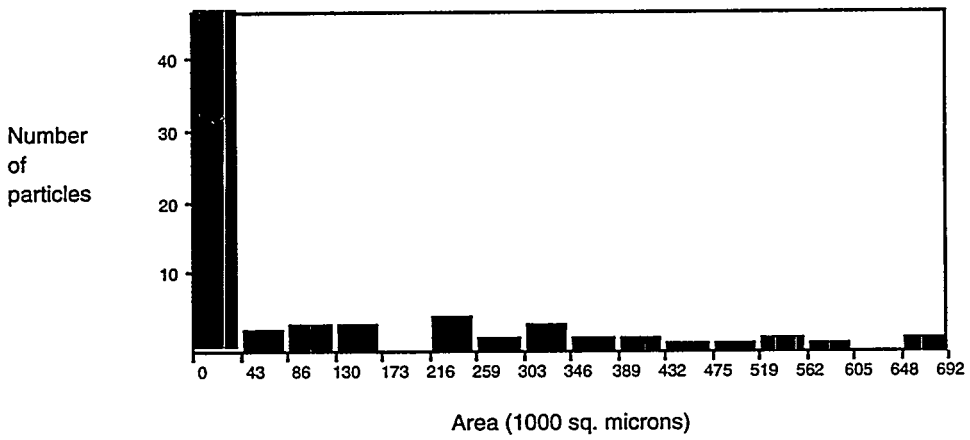

Fig. III-26. Particle Distribution of Resorcinol Sample in Fig. III-24 as Function of Area (average value, 60,000 μm)

The particles in the resorcinol sample after 10 cycles of irradiation are very tightly packed (Fig. III-27). This makes it difficult to determine the size distribution. It was necessary to separate particles using the software when a natural break (gain boundary contact) was suggested by the micrograph (Figs. III-28 and III-29).

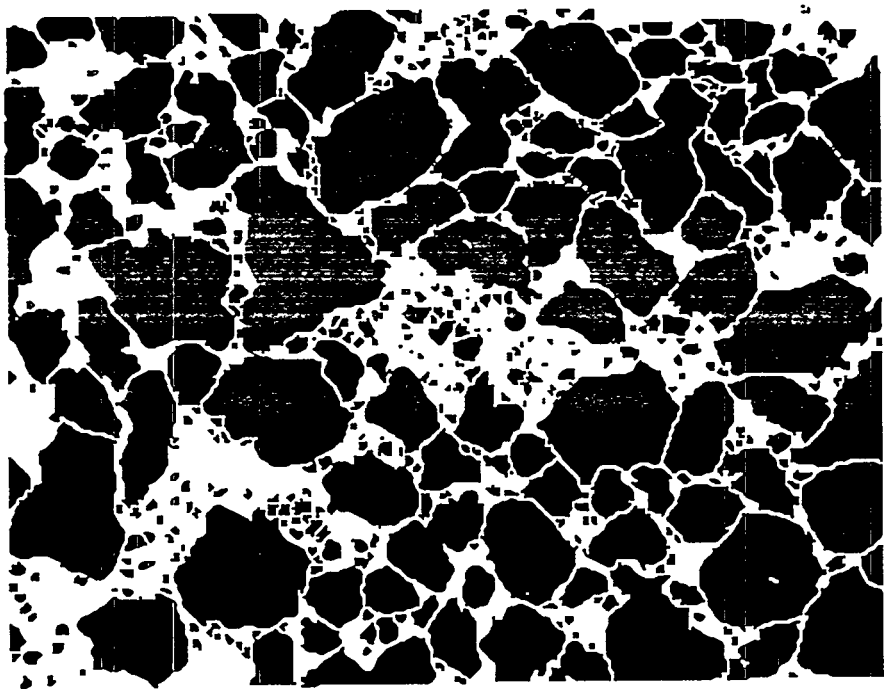

Fig. III-27. Micrograph of Resorcinol Sample (US form) after 10 Cycle Irradiation

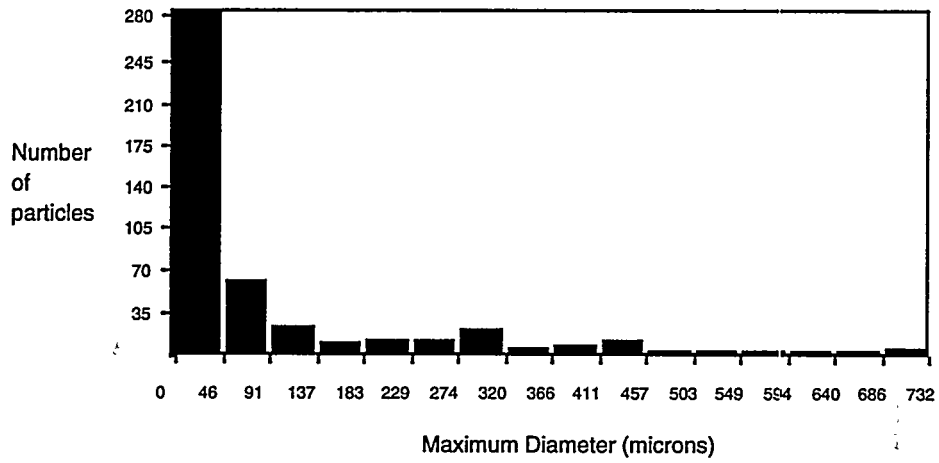

Fig. III-28. Particle Distribution of Resorcinol Sample in Fig. III-27 as Function of Diameter (average value, 95 μm)

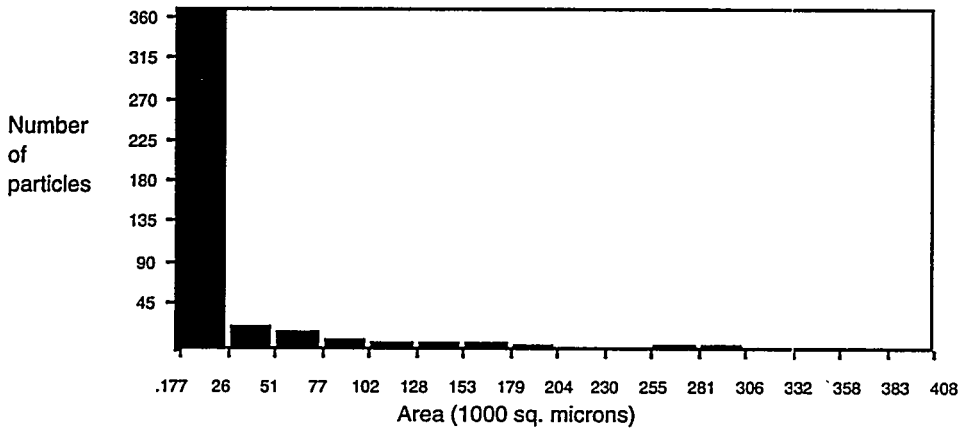

Fig. III-29. Particle Distribution of Resorcinol Sample in Fig. III-27 as Function of Area (average value, 21,000 μm^2)

In the micrograph of the resorcinol sample after the 100 cycle irradiation (Fig. III-30), the number of fine particles increased compared with Figs. III-24 and III-27. This suggests that the irradiation is breaking up the particles and creating these tiny fragments (fines), which may or may not have magnetite and cesium-extraction components (Figs. III-31 and III-32).

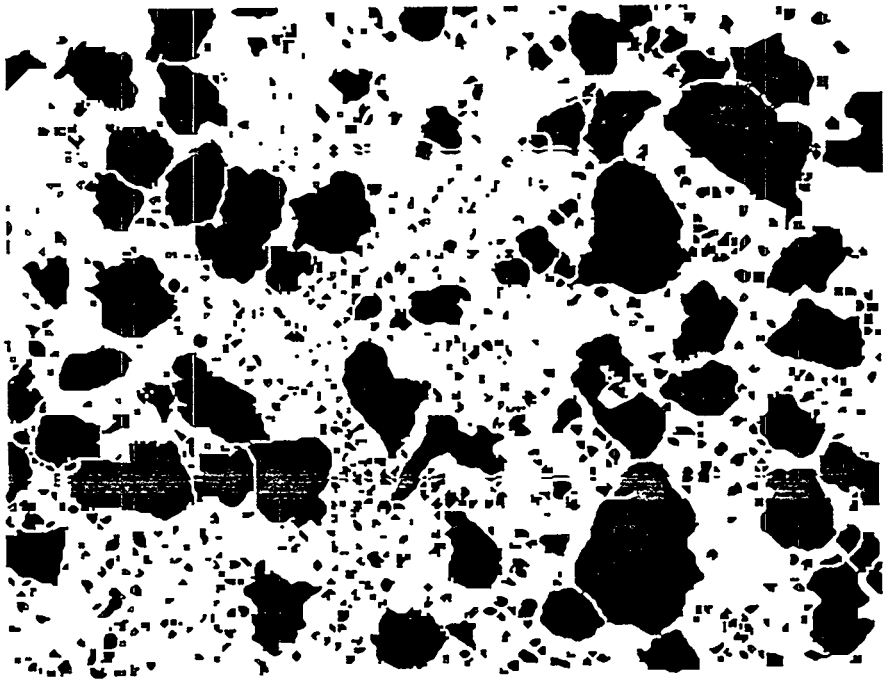

Fig. III-30. Micrograph of Resorcinol Sample (US form) after 100 Cycles

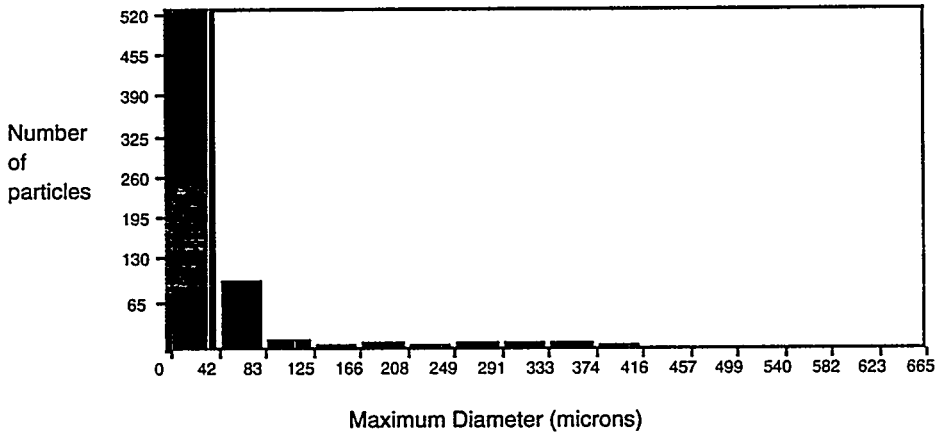

Fig. III-31. Particle Distribution of Resorcinol Sample in Fig. III-30 as Function of Diameter (average value, 55 μm)

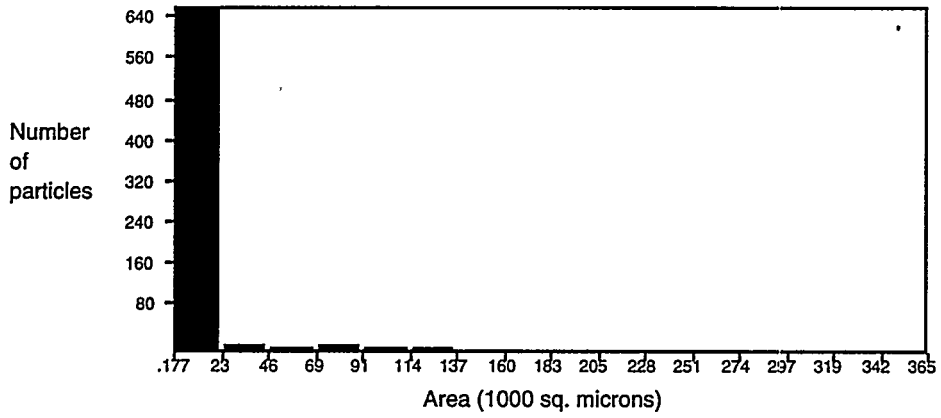

Fig. III-32. Particle Distribution of Resorcinol Sample in Fig. III-30 as Function of Area (average value, 8000 μm^2)

3. Conclusion

The overall effect of gamma radiation on the silico-titanate particles was a drastic increase in the particle size. This will cause a significant decrease in extraction efficiency due to the decreased surface area.

The resorcinol (US form) was also greatly affected by the radiation. As the irradiation dose increased, the number of smaller particles or fines increased. These smaller fragments may or may not have both the magnetic- and cesium-extracting components.

For the entire sample, the extent of the radiation damage and its result on the extraction efficiency cannot be determined; however, it is obvious through K_d measurements that the irradiation of the particles is decreasing their extraction performance.

APPENDIX A.

GAMMA IRRADIATION FACILITY

Facility Description

The gamma facility is located in the Chemistry Division at ANL. The gamma cell is approximately 4.3 m x 4.9 m (14 ft x 16 ft), with a 0.3 m (12.5 in.) ceiling. Most of the cell shown in Fig. A-1 can be used to irradiate samples depending on the dose requirements. All the reserved areas in Fig A-1 are available for short-term experiments such as particle irradiation (time frame of a few months). The atmosphere is once-through air, with a total of 34 m^3/min (1200 cfm) being exhausted. This produces an air change about every two minutes. The cobalt source is stored under the floor of the cell when not in use. The source is drawn out of the floor by means of an "A" frame mechanism to expose items placed in the cell. The shielding walls are 1.2-m (3.7-ft) thick magnetite concrete and should shield against 1 MCi of 1 MeV gamma energy. Viewing into the cell is provided by two zinc bromide windows, which normally are covered with six-inch shielding shutters. The shutters can be raised for a short time during irradiations to make observations.

Cobalt Source

The source array is comprised of six rods, 2.5-cm (1-in.) dia by 20-cm (8-in.) length. Four of the rods are located on a 6.3-cm (2.5-in.) radius from the center of the array. The other two rods are located on a 9.5-cm (3.75-in.) radius from the center of opposing corners of the array. The rods, when raised into the cell, are 40.6 cm (16 in.) from the floor to the centerline of the rod length. The original strength of the source was 70,000 Ci of cobalt-60 as of November 1990. There is a 0.8% reduction in strength per month.

Dosimeter

Dosimetry in the facility is performed using cobalt-doped glass dosimeters. The glass plate absorbency at 450 μm is measured before and after irradiation, and the difference in absorbency is used to determine absorbed doses. The glass plates have been calibrated against a ferrous sulfate dosimeter to determine the calibration curve for the glass. The response of the glass is linear from 1×10^5 to 5×10^6 rads. Dosimetry runs are timed to fall in this linear portion of the curve. The plates are read immediately after irradiation so that no corrections are necessary for fade characteristics. The accuracy of the glass dosimeter is ±10%.

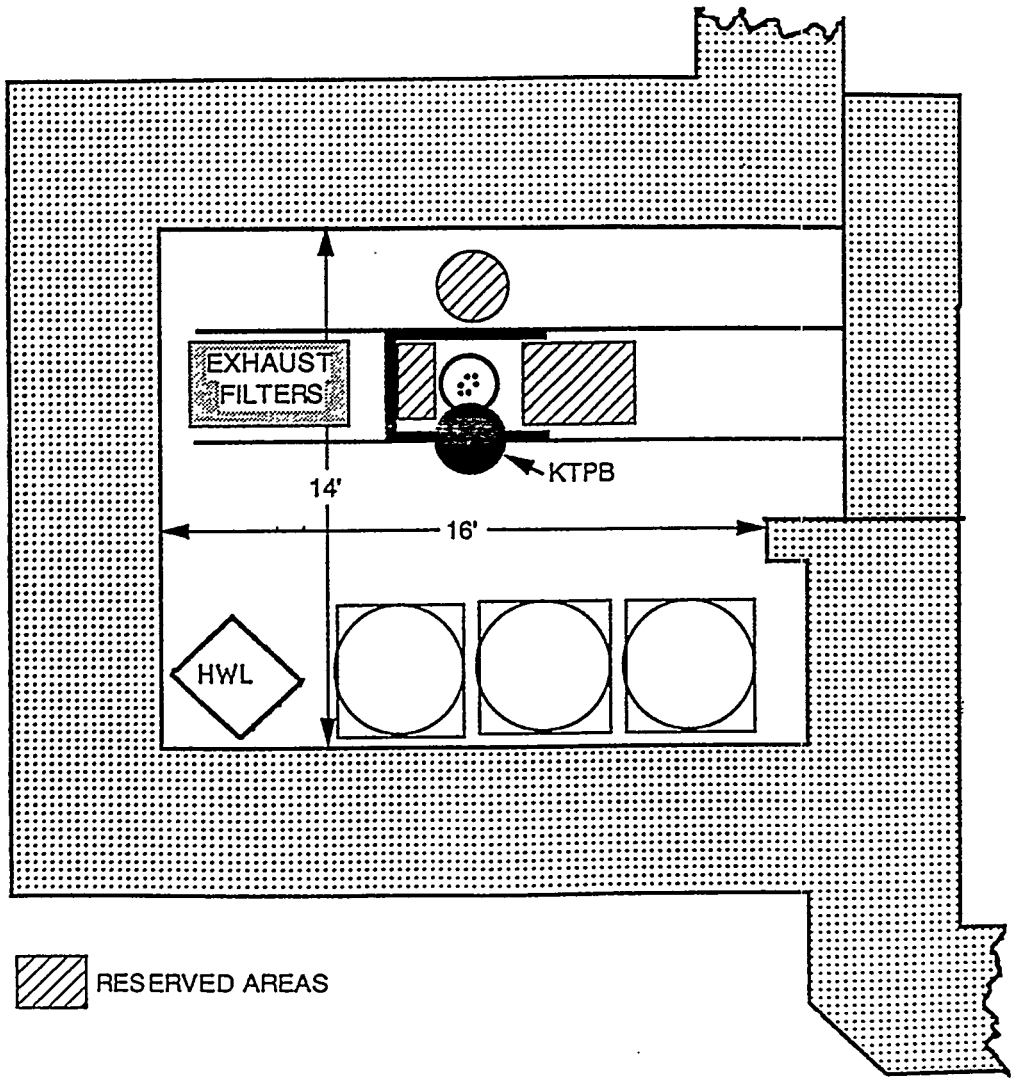

Fig. A-1. Layout of Gamma Facility

REFERENCES

1. H. Cember, *Introduction to Health Physics*, 2nd Ed., Pergamon Press, New York, pp. 97-131 (1988).

Distribution for ANL-94/47

Internal:

S. Asse
J. E. Battles
B. A. Buchholz
G. Dyrkacz
J. E. Harmon
M. D. Kaminski
J. J. Laidler
L. Nunez (20)
M. J. Steindler
C. E. Till
H. E. Tuazon
G. F. Vandegrift
TIS Files

External:

DOE-OSTI (2)
ANL-E Library (2)
ANL-W Library
Manager, Chicago Operations Office, DOE
J. Haugen, DOE-CH
Chemical Technology Division Review Committee Members:
- E. R. Beaver, Monsanto Company, St. Louis, MO
- D. L. Douglas, Consultant, Bloomington, MN
- R. K. Genung, Oak Ridge National Laboratory, Oak Ridge, TN
- J. G. Kay, Drexel University, Philadelphia, PA
- G. R. St. Pierre, Ohio State University, Columbus, OH
- J. Stringer, Electric Power Research Institute, Palo Alto, CA
- J. B. Wagner, Arizona State University, Tempe, AZ

K. J. Atkins, Bradtec, Inc., Atlanta, GA
F. M. Bos, Bradtec, Inc., Atlanta, GA
C. R. Bradley, Bolingbrook, IL
P. Colton, Pacific Northwest Laboratory, Richland, WA
G. R. Elder, Bradtec, Inc., Atlanta, GA
T. Fryberger, USDOE, Office of Environmental Management, Germantown, MD
W. L. Kuhn, Battelle Pacific Northwest Laboratory, Richland, WA
C. A. Swift, Bradtec, Inc., Atlanta, GA
I. R. Tasker, Waste Policy Institute, Gaithersburg, MD
J. Watson, Oak Ridge National Laboratory, Oak Ridge, TN